

Application of Real-World Modulation Schemes to Advanced Spatial Modulation Systems

by

Ahmad Bin Khalid

Supervised by:
Dr Tahmid Quazi
Prof. Hongjun Xu



A dissertation submitted in fulfilment for the degree of
Master of Science in Electronic Engineering

Discipline of Electrical, Electronic and Computer Engineering,
College of Agriculture, Engineering and Science,
University of KwaZulu-Natal, Durban, South Africa

February 2022

Declaration of Authorship

I, **Ahmad Bin Khalid**, declare that this dissertation titled, ‘**Application of Real-World Modulation Schemes to Advanced Spatial Modulation Systems**’ and the work presented in it are my own. I confirm that:

- The research reported in this dissertation, except where otherwise indicated, is my original work.
- This dissertation has not been submitted for any degree or examination at any other university.
- This dissertation does not contain other persons’ data, pictures, graphs or other information, unless specifically acknowledged as being sourced from other persons.
- This dissertation does not contain other persons’ writing, unless specifically acknowledged as being sourced from other researchers. Where other written sources have been quoted, then: i) their words have been re-written but the general information attributed to them has been referenced and ii) where their exact words have been used, their writing has been placed inside quotation marks, and referenced.
- Where I have reproduced a publication of which I am an author, co-author or editor, I have indicated in detail which part of the publication was written by myself alone and have fully referenced such publications.
- This dissertation does not contain text, graphics or tables copied and pasted from the Internet, unless specifically acknowledged, and the source being detailed in the dissertation and in the References sections.

Signed:

Date: **03 February 2022**

As the candidate’s supervisor, I, **Tahmid Quazi**, agree to the submission of this dissertation.

Signed:

Date:

Abstract

Multi-input multi-output (MIMO) technology is an essential part of the current and the next generation of wireless communication systems. Massive MIMO, an extension of MIMO, improves the throughput of traditional MIMO systems by introducing “massive” number of antennas. This invention forms an integral part of the development process from current to future wireless communication systems. Massive MIMO, which is also known as large-scale MIMO, utilizes the advancements made in the conventional MIMO systems in order to increase throughput and reliability. One such significant advancement is referred to as the Spatial Modulation (SM) technique. This technique utilizes the spatial domain to improve transmission rates and spectral efficiency of these multi-antenna systems. Further improvements on SM systems led to the introduction of the Generalised SM (GSM) technique. GSM, focussed on improving the spectral efficiency of SM-MIMO systems. However, for identical system configurations, the average bit error rate (BER) performance of GSM was limited compared to SM. This triggered extensive research on improving the BER performance of GSM-MIMO systems which led to the development GSM with constellation reassignment (GSM-CR). The first contribution of this dissertation is to propose the novel CR technique which maximises the Euclidean distance between transmitted symbol pairs to improve the BER performance of GSM-MIMO systems. At a BER of 10^{-5} , the systems 16-APSK GSM-CR and 32-APSK GSM-CR achieve a gain of 2.5dB and 2dB respectively over their equivalent GSM systems.

SM, GSM and GSM-CR techniques to date have largely been applied using M -ary Quadrature Amplitude Modulation (M -QAM) schemes. However, there are some drawbacks to these square or rectangular modulation schemes. One of which, when compared to circular constellation schemes, is the relatively higher peak-to-average power ratio (PAPR) in the transmitted signal. This results in significant reduction in the power amplifier’s efficiency as it is required to operate at a backed-off power level. Thus, the second contribution of this dissertation is to apply circular constellations, in particular Amplitude phase shift keying (APSK) modulation to the existing SM, GSM and GSM-CR systems. Analytical bound for the average BER for the proposed M -APSK SM, M -APSK GSM and M -APSK GSM-CR systems over fading channels is derived herein. Furthermore, a modified genetic algorithm is proposed to produce the secondary mappers for the M -APSK GSM-CR system. The analytical bounds derived for these systems are verified using Monte Carlo simulation results.

Acknowledgements

First of all, I would like to thank the God Almighty for everything He has provided me although no amount of gratitude is enough for all the bounties and favours He has bestowed upon me. I wish to express my deepest gratitude to all those that motivated me to complete this work especially my parents and my wife. Specials thanks to Dr. Tahmid Quazi, Prof. Hongjun Xu and Dr. Sulaiman Patel for all their guidance and unwavering support. Finally, I also wish to thank David Eagle for encouraging and supporting me to get this over the line.

“Many quote knowledge, but few note it in mind.”

~ Ali ibn Abu-Ta’lib (R.A.)

Contents

Declaration of Authorship	i
Abstract	ii
Acknowledgements	iii
List of Figures	vi
List of Tables	vii
Abbreviations	viii
1 Research Background	1
1.1 Introduction	1
1.1.1 Motivation and Context	1
1.1.2 Research Aim and Objectives	4
1.2 Contributions	6
1.2.1 Organization of Dissertation	7
2 Conference Article	10
2.1 Abstract	11
2.2 Introduction	11
2.3 System Model	12
2.4 16-APSK and 32-APSK Constellations	14
2.5 Performance Analysis of M -APSK SM System	15
2.5.1 Analytical BER of Symbol Estimation in AWGN (P_d)	15
2.5.2 Analytical BER of Symbol Estimation in Rayleigh Fading (P_d)	18
2.5.3 Analytical BER of Transmit Antenna Index Estimation (P_a)	19
2.6 Results and Discussion	20
2.7 Conclusion	21
3 Journal Article	24
3.1 Abstract	25
3.2 Introduction	25
3.2.1 Context of Research	25
3.2.2 Contributions	27
3.2.3 Structure and Notation	28

3.3	System Model	28
3.4	16-APSK and 32-APSK Constellations	30
3.5	BER Performance Analysis	31
3.5.1	Analytical BER of Transmit Antenna Index Estimation (P_a)	32
3.5.2	Analytical BER of Symbol Pair Estimation (P_d)	32
3.6	Constellation Reassignment Mapper Design	34
3.6.1	Description of Genetic Algorithm	35
	Genetic Coding	35
	Generating a Population of Chromosomes	36
	Crossover and Mutation	36
	Pruning	37
	Termination	37
	Implementation	38
3.7	Results and Discussion	38
3.8	Conclusion	41
3.9	Future Works	41
3.10	Appendix: Derivation of the Q -function Derivation	43
4	Conclusion	49

List of Figures

1.1	Block Diagram for the Alamouti System [12]	2
1.2	Block Diagram for the Labelling Diversity System [15]	3
1.3	Block Diagram for the Proposed Systems	5
2.1	System Model for M -APSK SM	12
2.2	APSK Constellations	13
2.3	Average BER - 6 bits/s/Hz Configuration	20
2.4	Average BER - 6 bits/s/Hz and 7 bits/s/Hz Configurations	21
2.5	Average BER - 7 bits/s/Hz and 8 bits/s/Hz Configurations	21
3.1	System Model for GSM-CR	28
3.2	GSM-CR Constellations, Key= ω_1/ω_2	31
3.3	Block Diagram of Genetic Algorithm for CR Mapper Design	35
3.4	Illustrating the position of Genes in M -APSK Constellations	36
3.5	Average BER - 6 bits/s/Hz Configuration	38
3.6	Average BER - 7 bits/s/Hz Configuration	39
3.7	Average BER - 7 bits/s/Hz Configuration	39
3.8	Average BER - 8 bits/s/Hz Configurations	40

List of Tables

3.1	PAPR of M -APSK and M -QAM constellations	38
3.2	$4 \times N_r$ Antenna Pairs	39
3.3	$6 \times N_r$ Antenna Pairs	40

Abbreviations

5G	Fifth Generation
AASC	Antenna Array Size and Configuration
APSK	Amplitude Phase Shift Keying
AWGN	Additive White Gaussian Noise
BEP	Bit Error Probability
BER	Bit Error Rate
BICM	Bit-Interleaved Coded Modulation
BS	Base Station
CR	Constellation Reassignment
CSI	Channel State Information
DSM	Differential Spatial Modulation
DVB-S2	Digital Video Broadcasting-Satellite-2nd Generation
ED	Euclidean Distance
EQSM	Extended Quadrature Spatial Modulation
GA	Genetic Algorithm
GSM	Generalised Spatial Modulation
GQSM	Generalised Quadrature Spatial Modulation
HSX	Hypersphere Swap Crossover
IAS	Inter-Antenna Synchronisation
ICI	Inter Channel Interference
MGF	Moment Generating Function
MIMO	Multiple-Input Multiple-Output
MLD	Maximum-Likelihood Detection
NCSM	Non-Coherent Spatial Modulation
NE	Non Equiprobable
PAPR	Peak-to-Average Power Ratio

PEP	P airwise E rror P robability
PSK	P hase S hift K eying
QAM	Q uadrature A mplitude M odulation
QSM	Q uadrature S patial M odulation
RF	R aleigh F ading
RV	R andom V ariable
SM	S patial M odulation
SNR	S ignal-to- N oise R atio
STBC	S pace- T ime B lock C ode
STLD	S pace- T ime L abelling D iversity
ST-QSM	S pace- T ime Q uadrature S patial M odulation
V-BLAST	V ertical- B ell L aboratories L ayered S pace- T ime

Chapter 1

Research Background

1.1 Introduction

1.1.1 Motivation and Context

Wireless communication systems are the backbone of the modern digitally connected world. The goal has been to continually improve wireless communication systems in terms of reliability and efficiency to seamlessly connect people anywhere and anytime. This led to the introduction of third and fourth generation wireless systems which provided improved range, reliability and data rate in comparison to their predecessors. However, there has been an exponential growth in the number of users that have adopted these wireless systems during the last decade. There are various reasons for such a growth, some of them include the availability of low-cost smartphone devices and affordable mobile data charges [1]. However, the requirement of these users were not being met due to the limitations in the 3G and 4G networks technologies. In order to satisfy the ever-increasing demands of the existing and new users, a fifth generation (5G) wireless system has been extensively researched in order to substantially improve the reliability and efficiency of its predecessors.

Furthermore, as countries imposed unprecedented restrictions to everyday life to contain the spread of COVID-19, the capacity, reliability and performance of these wireless communication systems have become even more evident. The pandemic has further increased the reliance on these systems as individuals utilize them to stay virtually connected with each and other. More importantly it has allowed many businesses to continue being productive throughout this crisis. This has accelerated the use of digital technologies at an unprecedented rate and led to the wireless communication systems to maintain connectivity [1]. Since the beginning of the pandemic, the development of 5G wireless communication system is one such technology that has accelerated to accommodate the sudden surge in demand.

Spectral and energy efficiency are the most widely researched areas in the context of 5G wireless communication technology. Massive multiple-input multiple-output (MIMO) is one such advanced

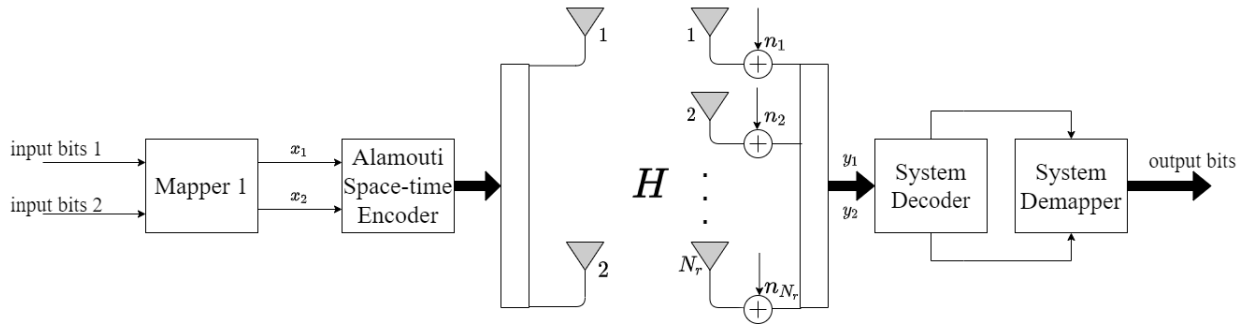


FIGURE 1.1: Block Diagram for the Alamouti System [12]

technology that has been developed to meet the requirement of the next generation of wireless communication systems. In this technology, the base station (BS) is incorporated with hundreds of antenna arrays which are used to create a reliable, high bandwidth connection [2]. Massive MIMO is foundationally built upon the advances made for conventional MIMO technology where in a significantly lower number of antennas are used [2]. In these conventional MIMO systems, diversity techniques are used to improve the overall link reliability of a wireless communication system. Diversity is achieved by sending the same information on multiple independent transmission paths and utilizing the multiple received signals for a more accurate detection [3].

One of the latest advances in the field of MIMO is the introduction of spatial modulation (SM) by Mesleh et al [4]. This novel transmission technique was developed to improve the transmission rates and spectral efficiency of MIMO systems. SM systems encode data in both the signal and spatial domains, in contrast to traditional techniques which are constrained to the signal domain. In the spatial domain, bits are used to indicate which of the N_t transmit antennas in the system is active during transmission. The benefits of this are twofold: 1) the spectral efficiency of the system increases by $\log_2(N_t)$ bits/sec/Hz, and 2) the use of only a single active transmit antenna eliminates the effects of inter-channel interference (ICI) and inter-antenna synchronisation (IAS) which are prevalent in MIMO systems[7].

The architecture of SM limits the number of information bits that may be encoded in the spatial domain since it only transmits using a single antenna. To further increase the spectral efficiency of SM systems, generalised spatial modulation (GSM) was proposed by Younis et al [7]. GSM systems optimise the encoding of information in the spatial domain, by selecting more than one antenna to be active in each time slot [7]. The overall spectral efficiency in GSM is improved by $\log_2(N_c)$, where N_c is the number of antenna combinations, compared to SM. Although the spatial domain is now improved, the reliability of GSM in comparison to SM is degraded due to the reintroduction of ICI. At BER of 10^{-5} , the 6 bits/s/Hz and 8 bits/s/Hz GSM systems are degraded by 0.5 dB in comparison to their equivalent SM systems [14]. A similar trend was also observed by Younis et al [7].

Several schemes have been developed to improve the reliability of traditional GSM systems [8–14]. These can be divided into two categories. The first category consists of closed-loop systems, which use

the channel state information (CSI) obtained from the receiver to optimize the transmission process. An example of this is the system proposed by Ma et al [8], which improves error performance by selecting the optimal signal-space constellation at the receiver according to CSI. The second category consists of open loop systems which do not utilize feedback [11, 12, 14, 15]. An example of such systems is the space-time block coded generalised spatial modulation (STBC-GSM) proposed by Basar et al [11]. In this scheme, the Alamouti structure was incorporated to improve the error performance over traditional GSM systems. The STBC system transmits multiple copies of the message signals over multiple transmit antennas and multiple time slots to improve the link reliability [12] (see Fig. 1.1).

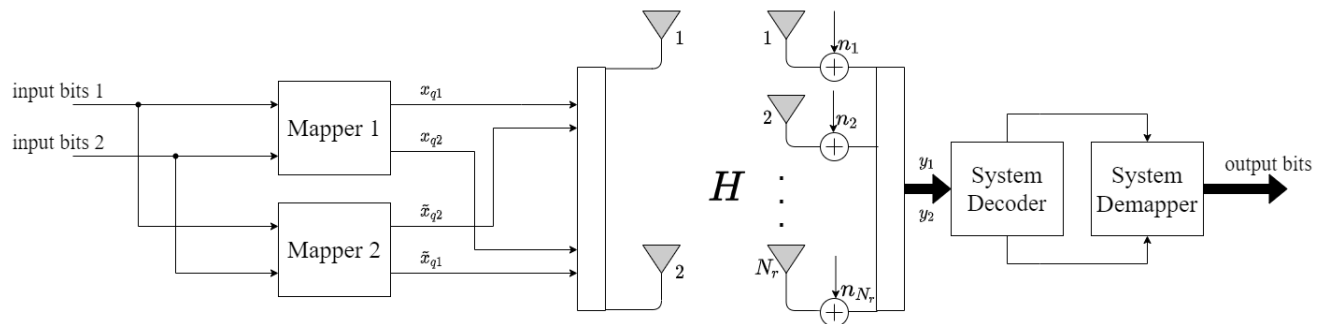


FIGURE 1.2: Block Diagram for the Labelling Diversity System [15]

More recently, labelling diversity (LD) as shown in Fig. 1.2 has been applied to GSM systems as a means to improve their error performance[15]. LD, which is an advancement of STBC, improves error performance by mapping the same information codewords using two bit-to-symbol mappers [15, 18, 19]. The application of LD to GSM system led to an introduction of GSM with constellation reassignment (GSM-CR) system [14]. The CR technique uses a single transmit timeslot system to improve the error performance of base GSM system [14]. These studies however, only discussed quadrature amplitude modulation (QAM) schemes. As an alternative, there are circular constellations, which have been widely accepted for systems such as satellite broadcasting [16]. One of the key advantages of circular constellations is that it leads to a lower peak-to-average power ratio (PAPR), when compared to square or rectangular modulation schemes such as M -QAM, where M is the modulation order. This is achieved by reducing the number of amplitude levels in circular constellations such as M -APSK constellations when compared to M -QAM with the same modulation order [21]. This property significantly reduces the design complexity of high-power amplifiers utilized in long-range wireless communication systems. Therefore, the focus of this dissertation is to implement SM, GSM and GSM-CR techniques with circular constellations, in particular, amplitude phase keying (APSK) modulation. APSK is the modulation scheme adopted for the latest digital video broadcasting (DVB-S2) standard, which provides the framework to improve transmission over non-linear satellite channels [16]. Thus, emphasizing the practicality and relevance of applying M -APSK constellations to SM, GSM and GSM-CR for potential use in long-range wireless communication systems.

The proposed M -APSK SM, GSM and GSM-CR systems offer two main technical challenges that are required to be overcome in order for their application. The first of them includes development of closed form expressions for the average BER for all three proposed systems. This requires an in-depth understanding of M -APSK constellations and the spatial modulation schemes in question. The second challenge includes the design of a secondary mapper given M -APSK mapper for the M -APSK GSM-CR system. This design is to ensure that adjacent symbols are spaced further apart in the secondary mapper than the primary mapper for an M order APSK modulation scheme.

1.1.2 Research Aim and Objectives

Advance MIMO techniques such as SM, GSM and GSM-CR to date have largely been applied to M -QAM schemes. Therefore, the aim of this dissertation is to apply circular constellations, in particular Amplitude phase shift keying (APSK) modulation to the existing SM, GSM and GSM-CR systems.

The first contribution of this research work focuses on the M -APSK SM system. This system was initially proposed by Li et al [6]. The authors present only simulation results of a single antenna configuration in order to study their proposed low complexity detection scheme. The results herein are not verified by a theoretical BER expression. In this dissertation, the performance study by Li et al. [6] is extended to include the derivation of a closed form expression for the average BER of an M -APSK SM system over fading channels. The theoretical expression derived is verified using multiple APSK constellations using various antenna configurations. The performance study in this dissertation includes results for a wider range of antenna configurations than that used in Li et al [6].

SM systems increase the spectral efficiency of the system over the traditional MIMO techniques such as vertical Bell Laboratories space-time (V-BLAST) and orthogonal STBC (OSTBC). However, the modulation efficiency is reduced rapidly as the number of transmit antennas are increased. This led to the introduction of GSM systems. The efficiency of GSM systems increases as the number of transmit antennas increase by activating more than one antenna during the transmission process. This makes GSM a promising technique for Massive MIMO in 5G wireless communication systems. By definition, Massive MIMO, which is an extension of conventional MIMO, fundamentally reaps all the benefits of conventional MIMO systems on a larger scale [17]. Given the motivation of improving throughput of SM systems with circular constellations, the focus of this dissertation then shifts on the application of M -APSK modulation scheme to GSM system in a conventional MIMO setting. A theoretical average BER is derived to verify the simulation results of M -APSK GSM system. Although the throughput and spectral efficiency is improved, the link reliability of the system is slightly degraded as compared to the M -APSK SM.

In recent years, significant research has been conducted in the development of GSM systems. The primary focus has been to improve the BER performance and/or throughput. Various BER performance enhancing techniques have been applied to GSM systems. The Alamouti STBC technique

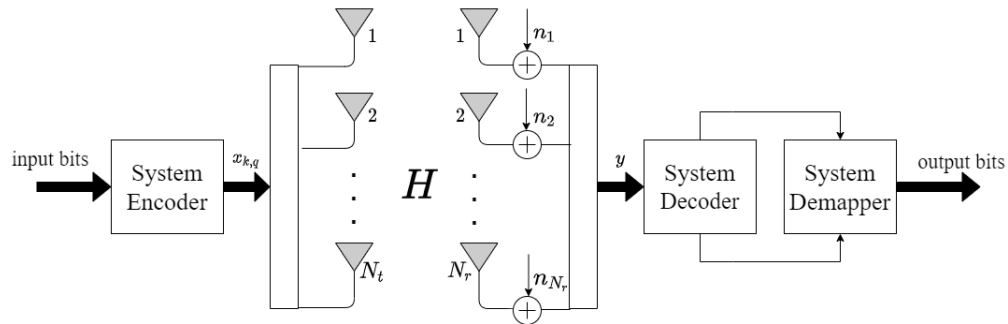


FIGURE 1.3: Block Diagram for the Proposed Systems

[5] as shown in Fig. 1.1, sends multiple copies of the message over multiple transmit antennas and multiple timeslots to increase the overall link reliability. Thereafter, LD was introduced by Xu et al [15] as an enhancement scheme to the Alamouti system to further improve the BER performance of MIMO systems. As shown in Fig. 1.2, the input information is mapped to two different bit-to-symbol mappers and sent over multiple transmit antennas and multiple timeslots. The improved BER performance is achieved by ensuring that adjacent symbols are spaced further apart in the secondary mapper than the primary mapper. The aim herein is to maximise the minimum Euclidean distance between symbol pairs in each constellation [15]. As a result, the detection at the receiver utilises symbol pairs instead of individual symbols. Although the complexity at the receiver increases, the enhanced error performance is achieved in the same manner as the conventional error correction codes [20]. Lastly, the CR technique which is a form of the LD technique achieves enhanced error performance over a single timeslot whereas the Alamouti STBC and base LD technique transmits information over multiple timeslots [14].

The resultant novel GSM-CR system [14] significantly improves the BER performance as compared to the conventional GSM system. However, the GSM-CR system, to date, has only been applied to square or rectangular modulation schemes. Since the primary goal of this dissertation is to apply circular constellations to advanced MIMO systems, the focus then shifts to developing an M -APSK GSM-CR system to improve the link reliability of M -APSK SM and M -APSK GSM systems. The theoretical average BER is also derived for this system to verify the simulation results. As hypothesised, the M -APSK GSM-CR system outperforms the equivalent M -APSK GSM and M -APSK SM systems. Fig. 1.3 outlines a generic block diagram that can be applied to all the proposed M -APSK SM, M -APSK GSM and M -APSK GSM-CR systems. The system encoder herein is adapted to implement each respective proposed system. The system encoder for each proposed system is discussed in the System Model section of Chapters 2 and 3 respectively. The channel conditions and receiver are set to be identical for all the proposed systems.

Based on the above motivation and aim, the objectives of this research work may be summarised as follows:

1. Apply circular constellations, in particular M -APSK, to SM, GSM and GSM-CR systems.
2. Derive a closed form expressions for the average BER for the M -APSK SM, M -APSK GSM and M -APSK GSM-CR systems.
3. Develop an algorithm that may be utilized to design secondary mappers for the APSK constellations for the CR system.
4. Provide a detailed performance study that includes the analyses of numerical and analytical results of the proposed systems for various system configurations.

1.2 Contributions

The research conducted in this dissertation has contributed towards a conference and a journal article respectively. The title, authors, article type, publication status and a short concise summary of these articles are provided below:

Article 1

Title	Performance Analysis of APSK in Spatial Modulation
Authors	Ahmad Khalid, Tahmid Quazi and Hongjun Xu
Type	Conference Article
Status	Published in <i>Proceedings of the Southern Africa Telecommunication Networks and Applications Conference (SATNAC) 2018</i> , Sep. 2018
Key Contributions	<ul style="list-style-type: none"> (a) A closed form expression for the average BER of an M-APSK SM system over fading channels. (b) Verification of the formulated analytical expressions using Monte Carlo simulations. (c) Performance study which presents the numerical and analytical results for the M-APSK SM system.

Article 2

Title	Performance Analysis of M -APSK Generalised Spatial Modulation with Constellation Reassignment
Authors	Ahmad Khalid, Tahmid Quazi, Hongjun Xu and Sulaiman Saleem Patel
Type	Journal Article
Status	Published in the <i>International Journal of Communication Systems</i> , 2020, vol 33, no.14, e-Locator e4497. DOI: 10.1002/dac.4497.
Key Contributions	<ul style="list-style-type: none">(a) The application of M-APSK to GSM and GSM-CR systems. The motivation for this being its lower PAPR when compared to M-QAM and its adoption in the DVB-S2 standard.(b) An analytical expressions to quantify the average bit error rate (BER) of M-APSK GSM and GSM-CR over fading channels.(c) The design of secondary mappers for the M-APSK GSM-CR system.(d) Verification of the formulated analytical expressions using Monte Carlo simulations.

1.2.1 Organization of Dissertation

The remainder of the dissertation is structured as follows:

Chapter 2 focuses on developing a theoretical expression for SM using 16-APSK and 32-APSK constellation in a Rayleigh fading (RF) channel. The theoretical average bit-error-rate (BER) expressions are compared to Monte Carlo simulation results. The performance study in this paper focuses on various system configurations.

Chapter 3 expands the study done in Chapter 2 from an M -APSK SM system to an application of M -APSK to GSM and GSM-CR systems. An analytical bound for the average bit error rate (BER) of the proposed M -APSK GSM and M -APSK GSM-CR systems over fading channels is derived. This chapter furthermore presents the numerical and analytical results for the proposed M -APSK GSM and GSM-CR systems.

Chapter 4 concludes the dissertation, highlights the contributions and briefly outlines possible future research work avenues.

References

- [1] K. Bahia and A. Delaporte, “The State of Mobile Internet Connectivity 2020,” Sep. 2020. [Online]. Available: <https://www.gsma.com/r/wp-content/uploads/2020/09/GSMA-State-of-Mobile-Internet-Connectivity-Report-2020.pdf>.
- [2] X. Kuai, X. Yuan, W. Yan, H. Liu, and Y. J. Zhang, “Double-Sparsity Learning-Based Channel-and-Signal Estimation in Massive MIMO with Generalized Spatial Modulation,” *IEEE Transactions on Communications*, vol. 68, no. 5, pp. 2863–2877, May 2020, doi: 10.1109/tcomm.2020.2969905.
- [3] S. Patel, “Uncoded Space-Time Labelling Diversity: Data Rate and Reliability Enhancements and Application to Real-World Satellite Broadcasting,” PhD Thesis, University of KwaZulu-Natal, 2019.
- [4] R. Y. Mesleh, H. Haas, S. Sinanovic, Chang Wook Ahn, and Sangboh Yun, “Spatial Modulation,” *IEEE Transactions on Vehicular Technology*, vol. 57, no. 4, pp. 2228–2241, Jul. 2008, doi: 10.1109/tvt.2007.912136.
- [5] S. M. Alamouti, “A Simple Transmit Diversity Technique for Wireless Communications,” *IEEE Journal on Selected Areas in Communications*, vol. 16, no. 8, pp. 1451–1458, 1998, doi: 10.1109/49.730453.
- [6] C. Li, Y. Huang, M. Di Renzo, J. Wang, and Y. Cheng, “Low-Complexity ML Detection for Spatial Modulation MIMO with APSK Constellation,” *IEEE Transactions on Vehicular Technology*, vol. 64, no. 9, pp. 4315–4321, Sep. 2015, doi: 10.1109/tvt.2015.2430855.
- [7] A. Younis, N. Serafimovski, R. Mesleh, and H. Haas, “Generalised Spatial Modulation,” in *2010 Conference Record of the Forty Fourth Asilomar Conference on Signals, Systems and Computers*, Nov. 2010, pp. 1498–1502.
- [8] N. Ma, A. Wang, C. Han, and Y. Ji, “Adaptive Joint Mapping Generalised Spatial Modulation,” in *2012 1st IEEE International Conference on Communications in China (ICCC)*, Nov. 2012, pp. 520–523.
- [9] Z. Yiğit and E. Başar, “High-rate Generalized Spatial Modulation,” in *2016 24th Signal Processing and Communication Application Conference (SIU)*, Jun. 2016, pp. 1117–1120.
- [10] Y. Zhou, D. Yuan, X. Zhou, and H. Zhang, “Trellis Coded Generalized Spatial Modulation,” in *2014 IEEE 79th Vehicular Technology Conference (VTC Spring)*, Jan. 2015, pp. 1–5.
- [11] E. Basar, U. Aygolu, E. Panayirci, and H. V. Poor, “Space-Time Block Coded Spatial Modulation,” *IEEE Transactions on Communications*, vol. 59, no. 3, pp. 823–832, Mar. 2011, doi: 10.1109/tcomm.2011.121410.100149.

-
- [12] K. Sundaravadivu and S. Bharathi, "STBC Codes for Generalized Spatial Modulation in MIMO Systems," in *2013 IEEE International Conference On Emerging Trends in Computing, Communication and Nanotechnology (ICECCN)*, Jun. 2013, pp. 486–490.
- [13] K. Govindasamy, H. Xu, and N. Pillay, "Space-time block coded spatial modulation with labeling diversity," *International Journal of Communication Systems*, vol. 31, no. 1, p. e3395, Sep. 2017, doi: 10.1002/dac.3395.
- [14] N. Naidoo, "Enhanced Performance and Efficiency Schemes for Generalised Spatial Modulation," PhD Thesis, University of KwaZulu-Natal, 2017.
- [15] H. Xu, K. Govindasamy, and N. Pillay, "Uncoded Space-Time Labeling Diversity," *IEEE Communications Letters*, vol. 20, no. 8, pp. 1511–1514, Aug. 2016, doi: 10.1109/lcomm.2016.2580503.
- [16] European Telecommunications Standards Institute, Digital Video Broadcasting (DVB); *Second Generation Framing structure, Channel Coding and Modulation Systems for Broadcasting, Interactive Services, News Gathering and Other Broadband Satellite Applications*. France: European Broadcasting Union, 2014.
- [17] M. Pappa, C. Ramesh, and M. N. Kumar, "Performance comparison of massive MIMO and conventional MIMO using channel parameters," in *2017 International Conference on Wireless Communications, Signal Processing and Networking (WiSPNET)*, 2017, pp. 1808–1812.
- [18] H. Samra, Z. Ding, and P. M. Hahn, "Symbol Mapping Diversity Design for Multiple Packet Transmissions," *IEEE Transactions on Communications*, vol. 53, no. 5, pp. 810–817, May 2005, doi: 10.1109/tcomm.2005.847132.
- [19] K. G. Seddik, A. S. Ibrahim, and K. J. Ray Liu, "Trans-Modulation in Wireless Relay Networks," *IEEE Communications Letters*, vol. 12, no. 3, pp. 170–172, Mar. 2008, doi: 10.1109/lcomm.2008.071734.
- [20] A. Goldsmith, *Wireless Communications*. Cambridge: Cambridge University Press, 2005.
- [21] T. Quazi and H. Xu, "BER Performance of a Hierarchical APSK UEP System over Nakagami-m Fading," *SAIEE Africa Research Journal*, vol. 107, no. 4, pp. 230–236, Dec. 2016, doi: 10.23919/saiee.2016.8532258.

Chapter 2

Conference Article

Performance Analysis of APSK in Spatial Modulation

Ahmad Khalid, Tahmid Quazi, Hongjun Xu

Published: *Southern Africa Telecommunication Networks and Applications
Conference 2018*

2.1 Abstract

Spatial Modulation (SM) is a recently developed multiple-input multiple-output (MIMO) technique aimed at improving data rates. The focus of this chapter is to apply amplitude phase shift keying (APSK) modulation scheme to SM. Previous bit error rate (BER) performance studies of M -APSK SM systems have only been presented using simulation results and were not verified by an analytical framework. In this chapter, a closed form theoretical expressions for SM using 16-APSK and 32-APSK constellations are derived in a Rayleigh fading (RF) channel. The theoretical average BER expressions are shown to have a tight bound in the high signal-to-noise ratio (SNR) region when compared to Monte Carlo simulation results. The theory expression verified the simulation results of a 6 bits/s/Hz system configuration presented in a previous study. The performance study in this paper is then extended by presenting theory and simulation results for 7 bits/s/Hz and 8 bits/s/Hz system configurations.

2.2 Introduction

MIMO is a recently developed technology for achieving high data rates and increased spectral efficiencies in multimedia communications. One of the latest MIMO techniques is spatial modulation (SM) which allows data to be encoded in both the spatial and signal domains, resulting in an increased throughput [1–3]. Another desirable property of SM over conventional MIMO systems is that it completely avoids the inter-channel interference (ICI) and inter-antenna synchronization (IAS) due to a single transmit antenna being active at a given time. Additionally, it results in reduced power consumption since only a single chain of frequency is utilized [4].

Most of the proposed SM systems in literature have focused on amplitude/phase modulation (APM) [1–6]. However, very few have considered circular constellations such as Star-QAM (Quadrature Amplitude Modulation) and APSK (Amplitude Phase Shift Keying) [7, 11]. One of the key advantages of circular constellations is that it leads to a lower peak-to-average power ratio (PAPR) when compared to square or rectangular modulation schemes such as M -ary QAM. This is achieved by the reduced number of amplitude levels in comparison to M -QAM constellations with the same modulation order [8]. This property makes circular constellations more appropriate for applications in satellite broadcasting systems. In particular, APSK, is the modulation scheme chosen for the latest DVB-S2 standard which provides the framework to improve transmission over non-linear satellite channels [10].

Recently, Li et al [11] applied APSK in SM with the above-mentioned motivations. The aim herein was to develop a low complexity detection scheme for the M -APSK SM system. Furthermore, it provided a bit error rate (BER) performance of the proposed system with a 4×2 antenna configuration. However, the results presented were only from simulations and were not verified using theoretical analysis. The aim of this chapter is to analyse the theoretical BER performance of the

M -APSK SM system and compare it to the simulation results. A closed form expression for the average BER is formulated for a fading channel. The performance study is extended by presenting results for a wider range of antenna configurations than that used in Li et al [11].

In terms of notation, this chapter represents vectors and scalars in boldface and italics respectively. $\|\cdot\|$, $|\cdot|$ and $E\{\cdot\}$ represent the Frobenius norm of a vector, the absolute value of a complex number and statistical expectation, respectively. The rest of the chapter is organized as follows. Section II details the system model for a M -APSK SM system. Section III outlines the constellations utilized. The theoretical BER expressions for the 16-APSK and 32-APSK constellations in SM are derived in Section IV. Section V presents the theoretical and simulation BER performance of the system. Finally, Section VI concludes the chapter.

2.3 System Model

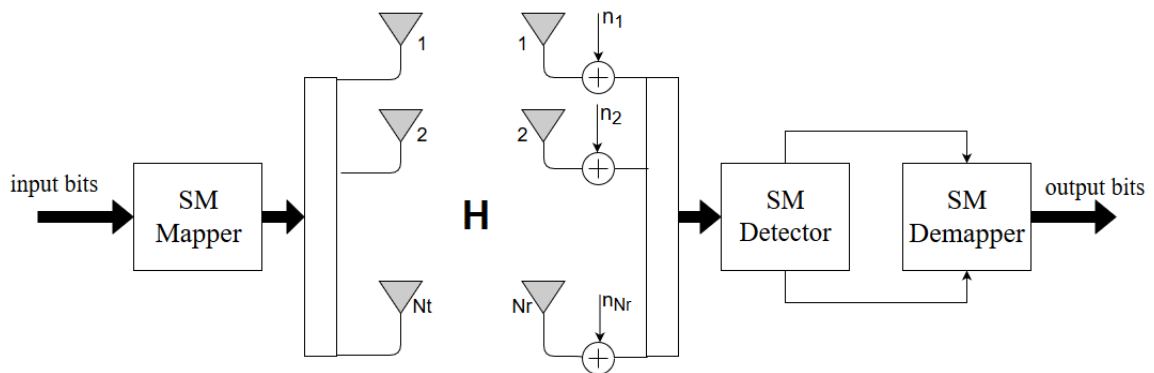


FIGURE 2.1: System Model for M -APSK SM

The $N_T \times N_R$ M -APSK SM system model is shown in Fig. 2.1, where N_T refers to number of transmit antennas and N_R is the number of receive antennas. The SM Mapper takes in an input stream of r bits which are mapped to a modulated symbol and a unique transmit antenna index.

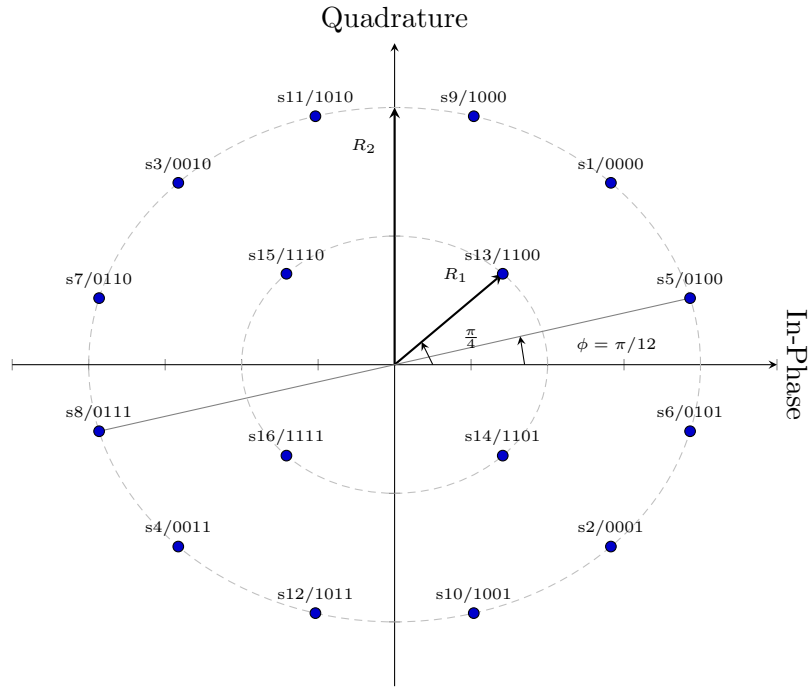
$$r = \log_2(MN_T), \quad (2.1)$$

where M denotes the order of the APSK modulation scheme.

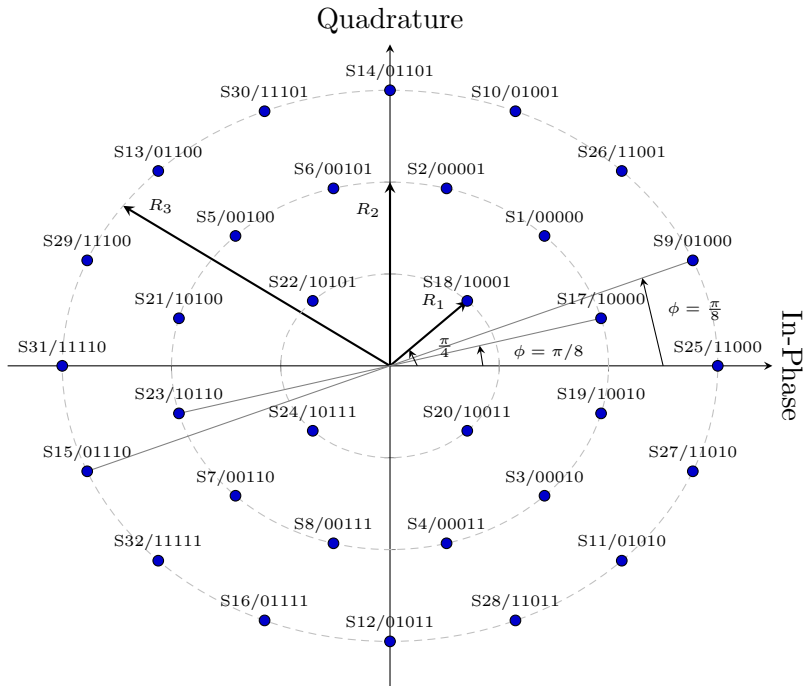
This assigning of bits is done using a predefined mapping table which is available at the transmitter and receiver. The outcome of the spatial and signal mapping processes can be expressed as follows:

$$x_{jq} = [0 \dots 0 \dots x_q \dots 0 \dots 0]^T, \quad (2.2)$$

where x_{jq} is $N_T \times 1$ vector, symbol x_q is q^{th} modulated symbol from an APSK constellation with $q \in [1 : M]$ and $E\{|x_q|^2\} = 1$. Symbol x_q is transmitted from antenna j over the $N_R \times N_T$ MIMO



(A) Constellation Representation of 16-APSK



(B) Constellation Representation of 32-APSK

FIGURE 2.2: APSK Constellations

channel \mathbf{H} , and also subjected to $N_R \times 1$ dimensional additive white Gaussian noise (AWGN) \mathbf{n} . The entries of \mathbf{H} and \mathbf{n} are independent and identically distributed (i.i.d) according to the complex Gaussian distribution $CN(0, 1)$.

The received signal vector is thus given by:

$$\mathbf{y} = \sqrt{\rho} \mathbf{H} x_{jq} + \mathbf{n}, \quad (2.3)$$

where \mathbf{y} is the $N_R \times 1$ dimensional received vector. $\mathbf{H} = [\mathbf{h}_1 \mathbf{h}_2 \dots \mathbf{h}_j \dots \mathbf{h}_{N_T}]$ and \mathbf{h}_j is the $N_R \times 1$ dimensional vector corresponding to transmit antenna j . ρ is the average SNR at each receive antenna.

The receiver employs the following ML detection rule for the estimation of transmit antenna index and the transmitted symbol:

$$[\tilde{j}, \tilde{q}] = \min_{\substack{j \in [1:N_T] \\ \hat{q} \in [1:M]}} \|\mathbf{y} - \sqrt{\rho} \mathbf{H} x_{j\hat{q}}\|_F^2, \quad (2.4)$$

where \tilde{j}, \tilde{q} represent the estimated transmitted antenna index and modulated symbol respectively.

2.4 16-APSK and 32-APSK Constellations

The modulation schemes in the DVB-S2 standard [10] are 16-APSK and 32-APSK. The constellation diagrams and the associated bit allocation for the two modulation schemes are shown in Fig. 2.2. In the 16-APSK constellation, the ratio of the outer and inner radii is denoted by $\beta_0 = R_2/R_1$ whilst the ratios in the 32-APSK constellation are defined as $\beta_1 = R_2/R_1$ and $\beta_2 = R_3/R_1$.

The average symbol energy for 16-APSK is calculated as follows:

$$\begin{aligned} \bar{E}_S &= \frac{(R_1^2 + 3R_2^2)}{4} = \frac{(1 + 3\beta_0^2)R_1^2}{4} \\ &= \alpha_0^2 R_1^2, \end{aligned} \quad (2.5)$$

where $\alpha_0 = (1 + 3\beta_0^2)/4$.

Similarly, the average symbol energy for 32-APSK is calculated as follows:

$$\begin{aligned} \bar{E}_S &= \frac{(R_1^2 + 3R_2^2 + 4R_3^2)}{8} = \frac{(1 + 3\beta_1^2 + 4\beta_2^2)R_1^2}{8} \\ &= \alpha_1^2 R_1^2, \end{aligned} \quad (2.6)$$

where $\alpha_1 = (1 + 3\beta_1^2 + 4\beta_1^4)/8$.

2.5 Performance Analysis of M -APSK SM System

The output of the SM detector shown in Fig. 2.1 estimates two quantities: the active transmit antenna index and the transmitted symbol. As a result, system performance depends on the error rates of these two parameters. Let P_a denote the probability of the transmit antenna index being incorrectly estimated given that the modulated symbol is correctly detected, and P_d be the probability of the modulated symbol being incorrectly estimated given that the transmit antenna index is correctly detected. The overall BER is then bounded by [1]:

$$P_e \leq 1 - P_c = P_a + P_d - P_a P_d, \quad (2.7)$$

where $P_c = (1 - P_a)(1 - P_d)$ is the error probability of SM bits being correctly detected.

2.5.1 Analytical BER of Symbol Estimation in AWGN (P_d)

The derivation starts by considering the symbol error rate (SER) of an M -ary modulation which is given by:

$$P_s(e) = \frac{1}{M} \sum_{i=1}^M P(e|s_i), \quad (2.8)$$

where $P(e|s_i)$ is the probability an error will occur if symbol s_i is transmitted. This is further given by:

$$P_s(e) = \frac{1}{M} \sum_{i=1}^M \sum_{j=1, j \neq i}^M P(s_i \rightarrow s_j), \quad (2.9)$$

where $P(s_i \rightarrow s_j)$ is the pairwise error probability (PEP) that s_i is transmitted and s_j is detected.

The union bound on the BER of M -ary modulation is obtained by modifying the SER in (2.9) to take into account the number of bits that will be in error for each PEP.

$$P_b(e) = \frac{1}{M} \sum_{i=1}^M \sum_{j=1, j \neq i}^M N(s_i, s_j) P(s_i \rightarrow s_j), \quad (2.10)$$

where $N(s_i, s_j)$ is the number of bits in error from symbol s_i to s_j .

Since the constellation shown in Fig. 2.2a is symmetrical over the in-phase and quadrature axes, the results obtained from any one quadrant can be used to extrapolate the results for the entire constellation [14]. Thus, using the symbols in the first quadrant, the SER for the 16-APSK modulation scheme can be written as:

$$P_s(e) = \frac{1}{4} \left(P(e|s_{13}) + 2(P(e|s_9) + P(e|s_1)) \right) \quad (2.11)$$

An upper bound is obtained by considering only the nearest neighbours for each PEP in (2.11). Thus, $P(e|s_{13})$ is given as:

$$\begin{aligned} P(e|s_{13}) &\leq P(s_{13} \rightarrow s_9) + P(s_{13} \rightarrow s_5) + P(s_{13} \rightarrow s_1) \\ &\quad + P(s_{13} \rightarrow s_{15}) + P(s_{13} \rightarrow s_{14}) \\ &= Q\left(\frac{d_{13,9}}{\bar{E}_s} \rho\right) + Q\left(\frac{d_{13,5}}{\bar{E}_s} \rho\right) + Q\left(\frac{d_{13,1}}{\bar{E}_s} \rho\right) \\ &\quad + Q\left(\frac{d_{13,15}}{\bar{E}_s} \rho\right) + Q\left(\frac{d_{13,14}}{\bar{E}_s} \rho\right), \end{aligned} \quad (2.12)$$

where \bar{E}_s for 16-APSK is defined in (2.5), ρ is the average SNR at each receive antenna, $d_{i,j}$, $i, j \in [1 : M]$ is the Euclidean distance between symbol i and symbol j and $Q(x)$ is the Gaussian function which is defined in Simon et al [15] as:

$$Q(x) = \frac{1}{\pi} \int_0^{\pi/2} \exp\left(\frac{-x^2}{2(\sin \theta)^2}\right) d\theta \quad (2.13)$$

In a similar manner, the PEP terms for both $P(e|s_9)$ and $P(e|s_1)$ are as follows:

$$\begin{aligned} P(e|s_9) &\leq P(s_9 \rightarrow s_{13}) + P(s_9 \rightarrow s_1) + P(s_9 \rightarrow s_{11}) \\ &= Q\left(\frac{d_{9,13}}{\bar{E}_s} \rho\right) + Q\left(\frac{d_{9,1}}{\bar{E}_s} \rho\right) + Q\left(\frac{d_{9,11}}{\bar{E}_s} \rho\right) \end{aligned} \quad (2.14)$$

$$\begin{aligned}
P(e|s_1) &\leq P(s_1 \rightarrow s_{13}) + P(s_1 \rightarrow s_9) + P(s_1 \rightarrow s_5) \\
&= Q\left(\frac{d_{1,13}}{\bar{E}_s}\rho\right) + Q\left(\frac{d_{1,9}}{\bar{E}_s}\rho\right) + Q\left(\frac{d_{1,5}}{\bar{E}_s}\rho\right)
\end{aligned} \tag{2.15}$$

Using distance relations, $d_{13,9} = d_{13,5}$, $d_{13,15} = d_{13,14}$ and $d_{9,1} = d_{5,1} = d_{9,11}$, (2.10) and (2.11), the BER for 16-APSK is expressed as:

$$\begin{aligned}
P_b(e) &\leq \frac{1}{4}Q(u_1\bar{\gamma}) + \frac{1}{4}Q(u_2\bar{\gamma}\rho) + \frac{1}{8}Q(u_3\bar{\gamma}) \\
&\quad + \frac{3}{8}Q(u_4\bar{\gamma}),
\end{aligned} \tag{2.16}$$

$$\begin{aligned}
\text{where } \bar{\gamma} &= \frac{\rho}{\bar{E}_s}, u_1 = \frac{\beta_0^2 - \beta_0 + 1}{2\alpha_0}, u_2 = \frac{(\beta_0^2 - 1)^2}{2\alpha_0}, \\
u_3 &= \frac{1}{\alpha_0}, u_4 = \frac{2\beta_0^2(\sin \frac{\pi}{12})^2}{2\alpha_0}.
\end{aligned}$$

The process for deriving the 32-APSK BER is the same as that in the 16-APSK case. For the sake of brevity, the full derivation is omitted, and the final expression is defined as:

$$\begin{aligned}
P_b(e) &\leq \frac{1}{10}Q(v_1\bar{\gamma}) + \frac{1}{10}Q(v_2\bar{\gamma}) + \frac{1}{20}Q(v_3\bar{\gamma}) \\
&\quad + \frac{3}{20}Q(v_4\bar{\gamma}) + \frac{1}{5}Q(v_5\bar{\gamma}) + \frac{3}{20}Q(v_6\bar{\gamma}) \\
&\quad + \frac{1}{10}Q(v_7\bar{\gamma}) + \frac{1}{5}Q(v_8\bar{\gamma}),
\end{aligned} \tag{2.17}$$

$$\begin{aligned}
\text{where } \bar{\gamma} &= \frac{\rho}{\bar{E}_s}, v_1 = \frac{\beta_1^2 - \beta_1 + 1}{2\alpha_1}, v_2 = \frac{(\beta_1^2 - 1)^2}{2\alpha_1}, v_3 = \frac{1}{\alpha_1} \\
v_4 &= \frac{2\beta_1^2(\sin \frac{\pi}{12})^2}{2\alpha_1}, v_5 = \frac{\beta_1^2 - \beta_2^2 - 2\beta_1\beta_2 \cos \frac{\pi}{24}}{2\alpha_1}, \\
v_6 &= \frac{(\beta_2^2 - \beta_1^2)^2}{2\alpha_1}, v_7 = \frac{\beta_1^2 - \beta_2^2 - 2\beta_1\beta_2 \cos \frac{\pi}{12}}{2\alpha_1}, \\
v_8 &= \frac{\beta_1^2(1 - \cos \frac{\pi}{8})}{\alpha_1}.
\end{aligned}$$

2.5.2 Analytical BER of Symbol Estimation in Rayleigh Fading (P_d)

In a general Rayleigh fading (RF) channel model for a single-input single-output (SISO) system, the received signal, assuming that symbol s is being transmitted, is given by $r = \sqrt{\rho}hs + n$, where h is the fading channel coefficient and n is the AWGN component. If the received instantaneous SNR is defined as $\gamma = |h|^2\rho$, the probability density function (PDF) of γ is given by $f_\gamma(\gamma) = 1/\bar{\gamma} \exp(-\frac{\gamma}{\bar{\gamma}})$.

The BER for 16-APSK defined in (2.16) in a RF channel is given in Simon et al [15] as:

$$P_b(\bar{\gamma}) = \int_0^\infty P(e|\gamma)f_\gamma(\gamma)d\gamma, \quad (2.18)$$

In order to evaluate (2.18), an alternative expression for the Q -function will need to be used. The $Q(x)$ function is defined in (2.13).

Applying the trapezoidal rule provided for numerical integration to evaluate (2.13) leads to [16]:

$$Q(x) = \frac{1}{2n} \left(\frac{\exp(-\frac{x^2}{2})}{2} + \sum_{k=1}^{n-1} \exp\left(-\frac{x^2}{2(\sin \theta_k)^2}\right) \right), \quad (2.19)$$

where $\theta_k = k\pi/2n$ and n is the number of iterations. It is shown by Quazi [16] that choosing n greater than 6 results in sufficient accuracy in the numerical integration.

Defining the moment generating function (MGF) as $M(s) = \int_0^\infty \exp(s\gamma) \times f_\gamma(\gamma)d\gamma$, the MGF function for the RF pdf is given in Simon et al [15] as:

$$M(s) = \int_0^\infty \exp(-s\gamma) \times f_\gamma(\gamma)d\gamma = \frac{1}{1 + s\bar{\gamma}}, \quad (2.20)$$

Using (2.19) and (2.20), the average BER expression for N_R receive antennas for 16-APSK can be derived from (2.16) to be:

$$\begin{aligned}
P_d = P_b(\bar{\gamma}) &= \frac{1}{4n} \left(\frac{2}{(2 + u_1\bar{\gamma})} \right)^{N_R} + \frac{1}{2n} \sum_{k=1}^{n-1} \left(\frac{S_i}{S_i + u_1\bar{\gamma}} \right)^{N_R} + \\
&\frac{1}{8n} \left(\frac{2}{(2 + u_2\bar{\gamma})} \right)^{N_R} + \frac{1}{4n} \sum_{k=1}^{n-1} \left(\frac{S_i}{S_i + u_2\bar{\gamma}} \right)^{N_R} + \\
&\frac{1}{8n} \left(\frac{2}{(2 + u_3\bar{\gamma})} \right)^{N_R} + \frac{1}{4n} \sum_{k=1}^{n-1} \left(\frac{S_i}{S_i + u_3\bar{\gamma}} \right)^{N_R} + \\
&\frac{3}{8n} \left(\frac{2}{(2 + u_4\bar{\gamma})} \right)^{N_R} + \frac{3}{4n} \sum_{k=1}^{n-1} \left(\frac{S_i}{S_i + u_4\bar{\gamma}} \right)^{N_R}, \tag{2.21}
\end{aligned}$$

where n is the number of iterations, $S_i = 2 \sin(\frac{k\pi}{2n})^2$, N_R is the number of receive antennas, $u_t, t \in [1 : 4]$ and $\bar{\gamma}$ are defined in (2.16).

The average BER for 32-APSK is derived using a similar manner. For ease of expression, function $\zeta(s)$ is defined as:

$$\zeta(s) = \frac{1}{4n} \left(\frac{2}{(2 + s\bar{\gamma})} \right)^{N_R} + \frac{1}{2n} \sum_{k=1}^{n-1} \left(\frac{S_i}{S_i + s\bar{\gamma}} \right)^{N_R}, \tag{2.22}$$

where n is the number of iterations, $S_i = 2 \sin(\frac{k\pi}{2n})^2$, N_R is the number of receive antennas and $\bar{\gamma}$ is defined in (2.17).

Thus, the average BER for 32-APSK in terms of $\zeta(s)$ is:

$$\begin{aligned}
P_d = P_b(\bar{\gamma}) &= 2\zeta(v_1) + \zeta(v_2) + \zeta(v_3) + 3\zeta(v_4) \\
&+ 2\zeta(v_5) + \zeta(v_6) + 2\zeta(v_7) + 4\zeta(v_8), \tag{2.23}
\end{aligned}$$

where $v_t, t \in [1 : 8]$ is defined in (2.17).

2.5.3 Analytical BER of Transmit Antenna Index Estimation (P_a)

The probability of a transmit antenna index being in an error given that the modulated signal is detected correctly can be obtained from Naidoo et al [12]. The analytical BER expression in a RF channel is as follows:

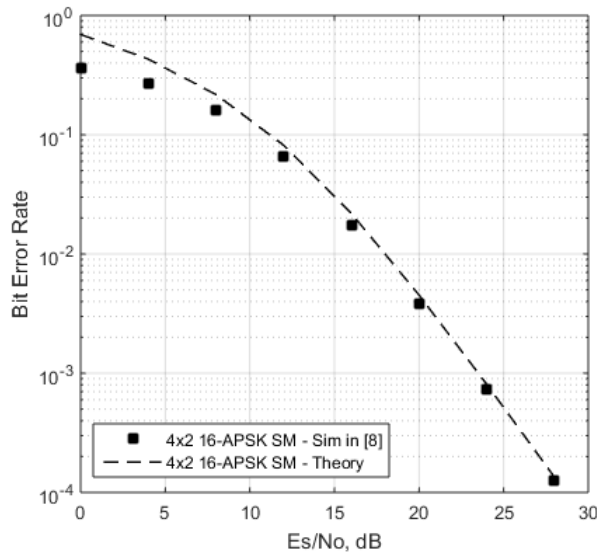


FIGURE 2.3: Average BER - 6 bits/s/Hz Configuration

$$P_a \leq \sum_{j=1}^{N_T} \sum_{q=0}^{M-1} \sum_{\hat{j}=1}^{N_T} \frac{N(j, \hat{j}) \mu_\alpha^{N_R} \sum_{w=0}^{N_R-1} \binom{N_R-1+w}{w} [1 - \mu_\alpha]^{N_R}}{N_T M}, \quad (2.24)$$

where $N(j, \hat{j})$ is the number of bits in error between antenna index j and \hat{j} , $\mu_\alpha = \frac{1}{2}(1 - \sqrt{\frac{\sigma_\alpha^2}{1+\sigma_\alpha^2}})$, $\sigma_\alpha^2 = (\rho/2)|x_q|^2$ and $q \in [1 : M]$ is the index of modulation scheme used.

2.6 Results and Discussion

This section presents the performance study conducted for the M -APSK SM system. The results were produced with 16-APSK constellation with $\beta_0 = 3.15$ and 32-APSK constellation with $\beta_1 = 2.58$ and $\beta_2 = 5.27$. Fig. 2.3 compares the simulations results of Li et al [11] in a 4×2 SM-16-APSK system with the results obtained from the theoretical BER expression (2.21) formulated in this chapter. As the graphs show, there is a good match between the two results plotted, thus verifying the closed form BER expression derived. The simulation results for the 4×2 SM-32-APSK system in Li et al [11] could not be replicated due to the details of the constellation design not being provided by the authors. However, the performance study was extended to 16-APSK and 32-APSK in multiple antenna configurations. Fig. 2.4 and Fig. 2.5 show the theory and simulation results for both constellations in a 4×4 and 8×4 antenna configurations, respectively. As expected, the union bound converges in the high SNR region thus verifying the analytical average BER expressions.

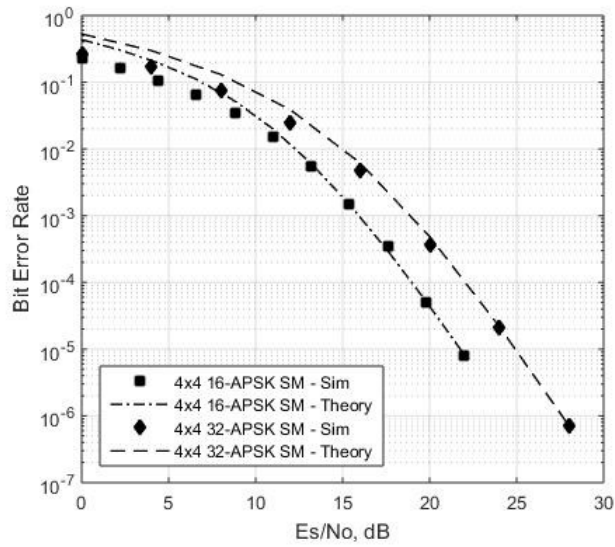


FIGURE 2.4: Average BER - 6 bits/s/Hz and 7 bits/s/Hz Configurations

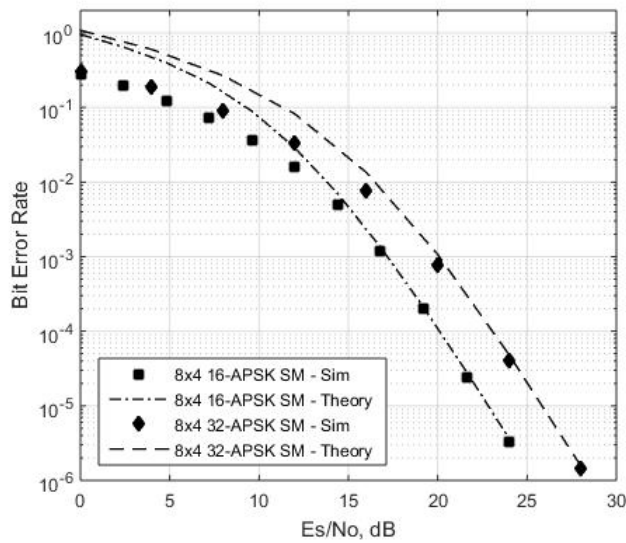


FIGURE 2.5: Average BER - 7 bits/s/Hz and 8 bits/s/Hz Configurations

2.7 Conclusion

This chapter presents a BER performance study for a M -APSK SM system. A closed form of the average BER theoretical expression for 16-APSK SM and 32-APSK SM is formulated. The theoretical expression for 16-APSK SM is shown to have a tight bound for the simulation results in a 4×2 system presented in a previous study. Furthermore, in this chapter, the results for 4×4 and 8×4 antenna configurations show that the theoretical expressions closely match simulation results. In future works, the theoretical expression will be used to study more advanced SM systems such as generalized spatial modulation (GSM).

References

- [1] R. Y. Mesleh, H. Haas, S. Sinanovic, Chang Wook Ahn, and Sangboh Yun, "Spatial Modulation," *IEEE Transactions on Vehicular Technology*, vol. 57, no. 4, pp. 2228–2241, Jul. 2008, doi: 10.1109/tvt.2007.912136.
- [2] M. Di Renzo, H. Haas, and P. M. Grant, "Spatial modulation for multiple-antenna wireless systems: a survey," *IEEE Communications Magazine*, pp. 182–191, 2011.
- [3] A. Stavridis, S. Sinanovic, M. Di Renzo, and H. Haas, "Energy Evaluation of Spatial Modulation at a Multi-Antenna Base Station," in *2013 IEEE 78th Vehicular Technology Conference (VTC Fall)*, 2014, pp. 1–5.
- [4] J. Jeganathan, A. Ghayeb, and L. Szczecinski, "Spatial modulation: Optimal Detection and Performance Analysis," *IEEE Communications Letters*, vol. 12, no. 8, pp. 545–547, Aug. 2008, doi: 10.1109/lcomm.2008.080739.
- [5] N. Pillay and H. Xu, "Low-complexity Transmit Antenna Selection Schemes for Spatial Modulation," *IET Communications*, vol. 9, no. 2, pp. 239–248, Jan. 2015, doi: 10.1049/iet-com.2014.0650.
- [6] H. Xu, "Simple low-complexity Detection Schemes for M-ary Quadrature Amplitude Modulation Spatial Modulation," *IET Communications*, vol. 6, no. 17, pp. 2840–2847, Nov. 2012, doi: 10.1049/iet-com.2012.0211.
- [7] P. Yang, Y. Xiao, B. Zhang, S. Li, M. El-Hajjar, and L. Hanzo, "Star-QAM Signaling Constellations for Spatial Modulation," *IEEE Transactions on Vehicular Technology*, vol. 63, no. 8, pp. 3741–3749, Oct. 2014, doi: 10.1109/tvt.2014.2306986.
- [8] T. Quazi and H. Xu, "BER Performance of a Hierarchical APSK UEP System over Nakagami-m Fading," *SAIEE Africa Research Journal*, vol. 107, no. 4, pp. 230–236, Dec. 2016, doi: 10.23919/saiee.2016.8532258.
- [9] Govindasamy K, Xu H, Pillay N. Space-time block coded spatial modulation with labeling diversity. *Int. J. Commun. Syst.* 2017;31(1):e3395. DOI: 10.1002/dac.3395.
- [10] Digital video broadcasting (DVB)-second generation framing structure, channel coding and modulation systems for broadcasting, interactive services, news gathering and other broadband satellite applications. 2014.
- [11] C. Li, Y. Huang, M. Di Renzo, J. Wang, and Y. Cheng, "Low-Complexity ML Detection for Spatial Modulation MIMO with APSK Constellation," *IEEE Transactions on Vehicular Technology*, vol. 64, no. 9, pp. 4315–4321, Sep. 2015, doi: 10.1109/tvt.2015.2430855.
- [12] N. R. Naidoo, H. J. Xu, and T. Al-Mumit Quazi, "Spatial modulation: Optimal Detector Asymptotic Performance and multiple-stage Detection," *IET Communications*, vol. 5, no. 10, pp. 1368–1376, Jul. 2011, doi: 10.1049/iet-com.2010.0667.

-
- [13] T. Quazi and H. Xu, “SSD-enhanced Uncoded space-time Labeling Diversity,” *International Journal of Communication Systems*, vol. 31, no. 11, p. e3592, May 2018, doi: 10.1002/dac.3592.
- [14] W. Sung, S. Kang, P. Kim, D.-I. Chang, and D.-J. Shin, “Performance Analysis of APSK Modulation for DVB-S2 Transmission over Nonlinear Channels,” *International Journal of Satellite Communications and Networking*, vol. 27, no. 6, pp. 295–311, May 2009, doi: 10.1002/sat.938.
- [15] M. K. Simon and M. Alouini, “A Unified Approach to the Performance Analysis of Digital Communication over Generalized Fading Channels,” *Proceedings of the IEEE*, vol. 86, no. 9, pp. 1860–1877, Sep. 1998, doi: 10.1109/5.705532.
- [16] T. Quazi, “Cross-layer Design for the Transmission of Multimedia Traffic over Fading Channels,” PhD Thesis, University of KwaZulu-Natal, 2009.

Chapter 3

Journal Article

Performance Analysis of M -APSK Generalised Spatial Modulation with Constellation Reassignment

Ahmad Khalid, Tahmid Quazi, Hongjun Xu and Sulaiman Saleem Patel

Published: *International Journal Communication Systems* 2020

2020, vol. 33, no. 14, e-locator e4497, DOI: 10.1002/dac.4497

3.1 Abstract

Generalised Spatial Modulation (GSM) is a recently developed multiple-input multiple-output (MIMO) technique aimed at improving data rates over conventional Spatial Modulation (SM) systems. However, for identical antenna array size and configurations (AASC), the bit error rate (BER) of GSM systems in comparison to SM systems is degraded. Recently, a GSM system with constellation reassignment (GSM-CR) was proposed in order to improve the BER of traditional GSM systems. However, this study focused on M -ary Quadrature Amplitude Modulation (M -QAM) schemes. The focus of this chapter is the application of a circular constellations scheme, in particular Amplitude phase shift keying (APSK) modulation, to GSM and GSM-CR systems. An analytical bound for the average BER of the proposed M -APSK GSM and M -APSK GSM-CR systems over fading channels is derived. The accuracy of this bound is verified using Monte Carlo simulation results. A 4×4 16-APSK GSM-CR system achieves a gain of 2.5 dB at BER of 10^{-5} over the traditional 16-APSK GSM system with similar AASC. Similarly, a 6×4 32-APSK GSM-CR system achieves a gain of 2 dB at BER of 10^{-5} over equivalent 32-APSK GSM system.

3.2 Introduction

3.2.1 Context of Research

Improving data rates and link reliability are key considerations for developing the next generation of wireless communication systems. These objectives led to the introduction of multiple-input multiple-output (MIMO) systems as an improvement to single antenna systems [1]. MIMO systems can be broken down into two broad categories. The first category focuses on multiplexing. An example of such a system is Vertical Bell Labs layered space-time (V-BLAST) [2], which attained high data rates by simultaneously transmitting independent information sequences. The spectral efficiency of such systems increased linearly with the number of transmit antennas being employed. The second category of MIMO systems focuses on achieving diversity. Alamouti was one of the first authors to introduce the MIMO space-time block coding (STBC) scheme, which attained transmit diversity [3]. Although, the overall link reliability was improved, the transmission rate remained the same as that achieved by single-input single-output (SISO) systems.

In order to improve the transmission rates and spectral efficiency of MIMO systems, spatial modulation (SM) was introduced as a new technique by Mesleh et al [4]. SM systems encode data in both the signal and spatial domains, in contrast to traditional techniques which are constrained to the signal domain. In the spatial domain, bits are used to indicate which of the N_t transmit antennas in the system is active during transmission. The benefits of this are twofold: 1) the spectral efficiency of the system increases by $\log_2(N_t)$ bits/sec/Hz, and 2) the use of only a single active transmit antenna eliminates the effects of inter-channel interference (ICI) and inter-antenna synchronisation (IAS) [5].

Architecture of SM however, limits the number of information bits that may be encoded in the spatial domain since it only transmits using a single antenna. To further increase the spectral efficiency of SM systems, generalised spatial modulation (GSM) was proposed by Younis et al [5]. GSM systems optimise the encoding of information in the spatial domain, by selecting more than one antenna to be active in each time slot [5]. The overall spectral efficiency in GSM is improved, by the base-two logarithm of the number of transmit antennas, compared to SM. Although the spatial domain is now optimised, the reliability of GSM in comparison to SM is degraded due to the reintroduction of ICI.

Several schemes have been developed in order to improve the reliability of traditional GSM systems [6–11, 13]. These can be divided into two categories. The first category consists of closed-loop systems, which use the channel state information (CSI) obtained from the receiver to optimize the transmission process. An example of this is the system proposed by Ma et al [6], which improves error performance by selecting the optimal signal-space constellation at the receiver according to CSI. The second category consists of open loop systems which do not utilize feedback [9, 10, 13, 14]. An example of such systems is the space-time block coded generalised spatial modulation (STBC-GSM) proposed by Basar et al [9]. In this scheme, the Alamouti structure was incorporated to improve the error performance over traditional GSM systems. More recently, labelling diversity (LD) has been applied to GSM systems as a means to improve their error performance. LD improves error performance by mapping the same information codewords using two bit-to-symbol mappers [14–16]. GSM with constellation reassignment (GSM-CR) [13] and GSM with space-time block coded modulation and labelling diversity (STBC-GSM-LD) [11] are examples of recent works that have applied LD to GSM systems. It is important to note that the CR technique utilized by Naidoo et al [13] only considers a single timeslot, whilst STBC-GSM-LD [14] transmits information bits over two timeslots. The utilization of a single timeslot results in lower latency and reduced detection complexity, at the expense of reduced error performance. This study however, only discussed quadrature amplitude modulation (QAM) schemes. The focus of this chapter is to implement GSM-CR with circular constellations, in particular, amplitude phase keying (APSK) modulation. One of the key advantages of circular constellations is that it leads to a lower peak-to-average power ratio (PAPR), when compared to square or rectangular modulation schemes such as M -QAM, where M is the modulation order. This is achieved as a result of the reduced number of amplitude levels in M -APSK constellations when compared to M -QAM with the same modulation order [17]. This property significantly reduces the design complexity of high-power amplifiers utilized in long-range wireless communication systems. This is highlighted by the fact that APSK is the modulation scheme adopted for the latest digital video broadcasting (DVB-S2) standard, which provides the framework to improve transmission over non-linear satellite channels [18]. Therefore emphasizing the practicality and relevance of applying M -APSK constellations to GSM and GSM-CR for potential use in long-range wireless communication systems.

Recently, a differential SM (DSM) system for APSK modulation schemes was proposed by Martin et al [19] to improve error performance over DSM for PSK systems. To further improve the link

reliability of SM systems, an optimal multi-ring APSK based non-coherent SM (NCSM) system assuming no CSI was proposed by Zhou et al [20]. In their letter Zhou et al designed APSK constellations based on the theoretical symbol error probability (SER) of the NCSM system. In related work, a novel non-equiprobable APSK (NE-APSK) constellation labelling for bit-interleaved coded modulation (BICM) systems was proposed [21]. The authors herein derive the NE-APSK design from Gray-APSK by reducing the number of points in the inner ring. Similarly, Yan et al [22] optimizes the parameters of Gray-APSK constellations for BICM systems using genetic algorithms (GAs). This is done by maximizing the channel capacity of the system. The resultant constellations in these works [19–22] however have some limitations that leave them unsuitable for the M -APSK GSM and GSM-CR systems proposed in this chapter: a) they are specifically designed for coded systems b) they deviate from the those recommended by the DVB-S2 standard.

The challenge of developing an M -APSK GSM-CR system is the design of a secondary mapper for a given M -APSK mapper. The objective of the design is to ensure that adjacent symbols are spaced further apart in the secondary mapper than the primary mapper. There are two approaches that are generally considered in order to design a secondary mapper. The first approach is to use geometric heuristics but to the best of the authors' knowledge, heuristics for generalised APSK constellations have yet to be introduced. The second approach is to search over all possible constellation assignments and select the one that maximizes the minimum Euclidean distance over all possible pairs of transmitted symbols [16]. This approach commonly referred to as an exhaustive search is highly complex and impractical, since it requires the system to consider $M!$ solutions where $(\cdot)!$ denotes the factorial function. In order to reduce the search space, Samra et al [15] presented a bounded search. Even after reducing the search space, Samra et al [15] reports that the algorithm is still too complex for constellations where $M \geq 16$. Most recently, a new approach to mapper design based on GAs was proposed by Patel et al [23, 24]. This algorithm allows for the design of mappers of higher modulation schemes, with feasible computational complexity. Thus, this algorithm is applied in this chapter to design the secondary mappers for the proposed M -APSK GSM-CR system.

3.2.2 Contributions

The principle contributions of this chapter are summarised as follows.

1. The application of M -APSK to GSM and GSM-CR systems. The motivation for this being its lower PAPR when compared to M -QAM and its adoption in the DVB-S2 standard.
2. An analytical expressions to quantify the average bit error rate (BER) of M -APSK GSM and GSM-CR over fading channels.
3. The design of secondary mappers for the M -APSK GSM-CR system.
4. Verification of the formulated analytical expressions using Monte Carlo simulations.

3.2.3 Structure and Notation

The remainder of this chapter is structured as follows. Sec. 3.3 details the system model for a M -APSK GSM-CR system. The theoretical BER expressions for M -APSK GSM-CR is derived in Sec. 3.5. Sec. 3.6 outlines the mapper design. Sec. 3.7 presents the theoretical and simulation BER performance of the system. Finally, Sec. 3.8 concludes the chapter.

In terms of notation, this chapter represents vectors and scalars in boldface and italics respectively. $\|\cdot\|_F$, $|\cdot|$ and $E\{\cdot\}$ represent the Frobenius norm of a vector, the absolute value of a complex number and statistical expectation respectively. The $\Re(\cdot)$ represents the real component of a complex signal. Lastly, $\lfloor \cdot \rfloor$ represents the floor function of a real number.

3.3 System Model

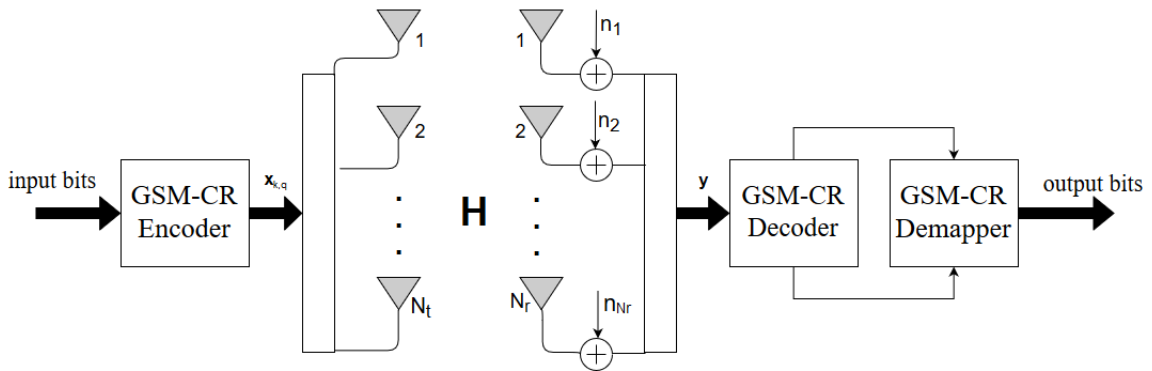


FIGURE 3.1: System Model for GSM-CR

The system considered in this chapter is an $N_t \times N_r$ M -APSK GSM-CR system as shown in Fig. 3.1, where N_t refers to the number of transmit antennas and N_r is the number of receive antennas. The encoder initially assigns a stream of $b = b_a + b_s$ information bits to a spatial symbol (consisting of b_a bits) and an M -APSK symbol (consisting of b_s bits). The selection of the transmit antennas refers to the spatial domain transmission whilst the selection of the symbol refers to the signal domain. In SM systems, the spatial domain utilizes a single antenna whereas GSM systems use a pair of antennas. The spatial domain consists of all the possible pairs of transmit antennas, where the indices of these pairs correspond to spatial symbols. There are $\binom{N_t}{2}$ ways to select an antenna pair from N_t transmit antennas. However, it should be noted that the number of usable antenna pair combinations must be an integer power of two. Thus, the number of antenna bits is given by $b_a = \lfloor \log_2 \binom{N_t}{2} \rfloor$. These bits define codeword c_a which are indexed by k where $k \in [0 : 2^{b_a} - 1]$. This antenna pair index defines the antenna pair $\{k_1, k_2\}$ to be used during transmission. The selection of these b_a antenna pairs for an $N_t \times N_r$ GSM system is discussed by Basar et al [9].

The signal domain in the GSM-CR system comprises of two symbols mapped by $b_s = \log_2 M$ bits, where M denotes the order of the APSK modulation scheme used. These bits are mapped to an M -APSK constellation using two bit-to-symbol mappers, primary mapper ω_1 and secondary mapper ω_2 . The output of these mappers are $x_q = \omega_1(q)$ and $\tilde{x}_q = \omega_2(q)$ where q represents the signal domain index and is defined by the range $[0 : M - 1]$. The output of the encoder shown in Fig. 3.1 can be expressed as:

$$\mathbf{x}_{k,q} = \left[0 \quad \dots \quad x_q \quad \dots \quad 0 \quad \dots \quad \tilde{x}_q \quad \dots \quad 0 \right]^T e^{j\theta_k} \quad (3.1)$$

where $\mathbf{x}_{k,q}$ is an $N_t \times 1$ dimensional transmission vector and θ_k is the rotation angle. Basar et al have presented the optimal transmit antenna pairs and the corresponding rotation angle for an $N_t \times N_r$ GSM system [9]. The same process has been applied for the proposed M -APSK GSM and M -APSK GSM-CR.

The power of the M -APSK constellation is normalized to ensure that $E\{|x_q|^2\} = E\{|\tilde{x}_q|^2\} = 1$. Modulated Symbols $x_q e^{j\theta_k}$ and $\tilde{x}_q e^{j\theta_k}$ are transmitted simultaneously from antennas k_1 and k_2 over the $N_r \times N_t$ MIMO channel \mathbf{H} .

The received signal vector is thus given by:

$$\mathbf{y} = \sqrt{\frac{\rho}{2}} \mathbf{H} \mathbf{x}_{k,q} + \mathbf{n}, \quad (3.2)$$

where \mathbf{y} is an $N_r \times 1$ dimensional received vector subjected to $N_r \times 1$ dimensional additive white Gaussian noise (AWGN) \mathbf{n} . The entries of \mathbf{H} and \mathbf{n} are independent and identically distributed (i.i.d) according to the complex Gaussian distribution $CN(0, 1)$. $\mathbf{H} = \left[\mathbf{h}_1 \quad \mathbf{h}_2 \quad \dots \quad \mathbf{h}_{k_1} \quad \dots \quad \mathbf{h}_{k_2} \quad \dots \quad \mathbf{h}_{N_t} \right]$ where \mathbf{h}_{k_1} and \mathbf{h}_{k_2} are the $N_r \times 1$ dimensional vectors corresponding to transmit antenna pair index k . ρ is the average signal-to-noise ratio (SNR) at each receive antenna.

Alternatively, the received vector for the APSK GSM-CR can be represented as:

$$\mathbf{y} = \sqrt{\frac{\rho}{2}} \mathbf{h}_k \mathbf{X}_q + \mathbf{n}, \quad (3.3)$$

where $\mathbf{X}_q = \left[x_q \quad \tilde{x}_q \right]^T e^{j\theta_k}$ is the transmitted symbol pair and $\mathbf{h}_k = \left[\mathbf{h}_{k_1} \quad \mathbf{h}_{k_2} \right]$ is an $N_r \times 2$ dimensional channel matrix corresponding to the active antenna pair index k .

The receiver employs the ML detection rule for the estimation of transmit antenna pair index and the transmitted symbol as shown in Eq. (3.4).

$$[\tilde{k}, \tilde{q}] = \min_{\substack{\hat{k} \in [0:2^{b_a}-1] \\ \hat{q} \in [0:M-1]}} \left\| \mathbf{y} - \sqrt{\frac{\rho}{2}} \mathbf{h}_{\hat{k}} \mathbf{X}_{\hat{q}} \right\|_F^2, \quad (3.4)$$

where \tilde{k}, \tilde{q} represent the estimated transmitted antenna pair index and M -APSK modulated index respectively.

3.4 16-APSK and 32-APSK Constellations

APSK constellations exist in multiple modulation schemes. These schemes are termed as $n_1 + n_2 + \dots + n_l$ APSK where l is the total number of rings and n_l is the number of points on the l^{th} ring. 4+12 APSK, 5+11 APSK, 6+10 APSK and 8+8 APSK are some of the common modulation schemes for 16-APSK. Among them, 4+12 APSK modulation scheme is proven to exhibit improved error performance, when considering the non-linear characteristics of a high performance amplifier [30–32]. Similar performance has been observed in 4-12-16 APSK (32-APSK) modulation scheme [30]. Furthermore, it is also worth mentioning that 4+12 APSK and 4+12+16 APSK are the chosen modulation schemes in the latest DVB-S2 standard for satellite communications over non-linear channels [18].

The constellation diagrams for 16-APSK and 32-APSK and the associated bit allocation for mappers ω_1 and ω_2 in decimal are shown in Fig. 3.2. In the 16-APSK constellation, the ratio of the outer and inner radii is denoted by $\beta_0 = R_2/R_1$ whilst the ratios in the 32-APSK constellation are defined as $\beta_1 = R_2/R_1$ and $\beta_2 = R_3/R_1$ [29].

The average symbol energy for 16-APSK is calculated as follows:

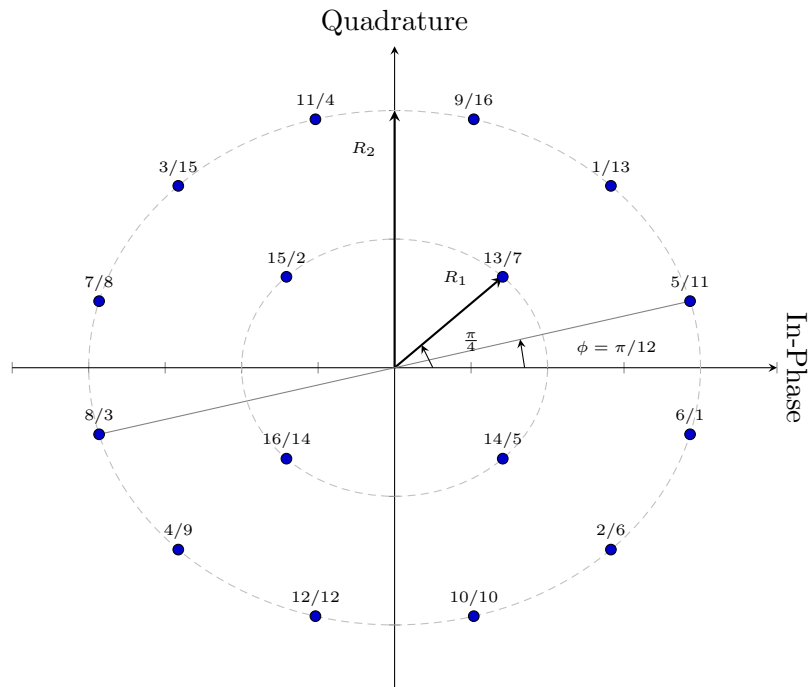
$$\begin{aligned} \bar{E}_S &= \frac{(R_1^2 + 3R_2^2)}{4} \\ &= \frac{(1 + 3\beta_0^2)R_1^2}{4} \end{aligned} \quad (3.5)$$

Similarly, the average symbol energy for 32-APSK is calculated as follows:

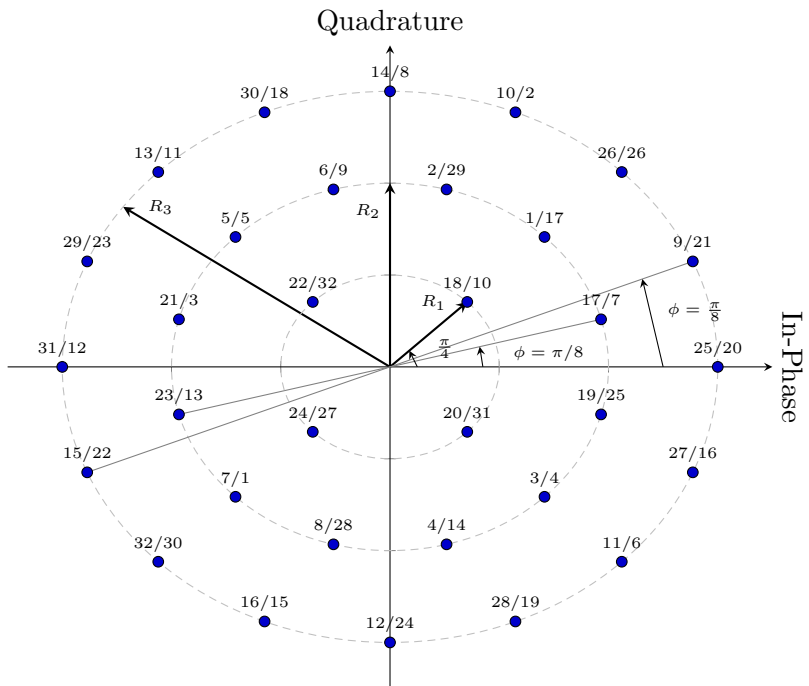
$$\begin{aligned} \bar{E}_S &= \frac{(R_1^2 + 3R_2^2 + 4R_3^2)}{8} \\ &= \frac{(1 + 3\beta_1^2 + 4\beta_2^2)R_1^2}{8} \end{aligned} \quad (3.6)$$

The peak-to-average power ratio may be calculated using the expression below [25]:

$$\text{PAPR} = 10 \log \left(\frac{\max_{q=0,1,\dots,M-1} |x_q|^2}{\frac{1}{M} \sum_{q=0}^{M-1} |x_q|^2} \right) \text{ dB} \quad (3.7)$$



(A) Constellation Representation of 16-APSK



(B) Constellation Representation of 32-APSK

FIGURE 3.2: GSM-CR Constellations, Key= ω_1/ω_2

3.5 BER Performance Analysis

The output of the GSM-CR detector, shown in Fig. 2.1, estimates two quantities: the active transmit antenna pair and the transmitted symbol. As a result, the system performance depends on the error rates of these two parameters. Let P_a denote the probability of the transmit antenna pair being incorrectly estimated, given that the modulated symbol pair is correctly detected, and P_d be

the probability of the modulated symbol pair being incorrectly estimated given that the transmit antenna pair is correctly detected. The overall average BER is then bounded by [4]:

$$P_e \approx P_a + P_d - P_a P_d \quad (3.8)$$

3.5.1 Analytical BER of Transmit Antenna Index Estimation (P_a)

The average BER for the transmit antenna index is calculated by assuming the transmitted signal is correctly detected. The closed-form solution is given by Naidoo et al[13] as:

$$P_a \leq \sum_{k=0}^{c-1} \sum_{q=0}^{M-1} \sum_{\substack{\hat{k}=0 \\ \hat{k} \neq k}}^{c-1} \frac{N(k, \hat{k}) \mu_\alpha^{N_R} \sum_{w=0}^{N_R-1} \binom{N_R-1+w}{w} [1 - \mu_\alpha]^{N_R}}{cM}, \quad (3.9)$$

where $N(k, \hat{k})$ is the number of bits in error between antenna pair indices k and \hat{k} , $\mu_\alpha = \frac{1}{2} \left(1 - \sqrt{\frac{\sigma_\alpha^2}{1 + \sigma_\alpha^2}} \right)$, $\sigma_\alpha^2 = (\rho/8)|x_q|^2$ where x_q is defined in Sec. 3.3 and $c = 2^{b_a}$.

3.5.2 Analytical BER of Symbol Pair Estimation (P_d)

The average BER of symbol estimation is derived using the union bound technique [27]. Assuming that the transmit antenna pair is correctly detected, the average BER for symbol pair estimation is bounded by[13]:

$$P_d \leq \sum_{q=0}^{M-1} \sum_{\substack{\hat{q}=0 \\ \hat{q} \neq q}}^{M-1} \frac{N(q, \hat{q}) P(\mathbf{x}_{k,q} \rightarrow \mathbf{x}_{k,\hat{q}})}{mM}, \quad (3.10)$$

where $m = \log_2 M$, $N(q, \hat{q})$ is the number of bit errors between symbol pair indices q and \hat{q} . $P(\mathbf{x}_{k,q} \rightarrow \mathbf{x}_{k,\hat{q}})$ denotes the pairwise error probability (PEP) of detecting $\mathbf{x}_{k,\hat{q}}$ given that $\mathbf{x}_{k,q}$ was transmitted.

The PEP conditioned on \mathbf{H} may be expressed as

$$P(\mathbf{x}_{k,q} \rightarrow \mathbf{x}_{k,\hat{q}} | \mathbf{H}) = P \left(\left\| \mathbf{y} - \sqrt{\frac{\rho}{2}} \mathbf{H} \mathbf{x}_{k,\hat{q}} \right\|_F^2 < \left\| \mathbf{y} - \sqrt{\frac{\rho}{2}} \mathbf{H} \mathbf{x}_{k,q} \right\|_F^2 \right) = \mathcal{Q} \left(\sqrt{\sum_{i=1}^{N_r} v_i} \right) \quad (3.11)$$

where $v_i = \frac{|u_i|^2}{2}$ and u_i is the i^{th} element of vector \mathbf{u} . $\mathbf{u} = \sqrt{\frac{\rho}{2}} [\mathbf{h}_{k_1} d_1 + \mathbf{h}_{k_2} d_2] e^{j\theta_k}$ where $d_1 = (x_q - x_{\hat{q}})$ and $d_2 = (\tilde{x}_q - \tilde{x}_{\hat{q}})$. The derivation of the \mathcal{Q} -function can be found in Appendix 3.10.

In order to evaluate Eq. (3.11), the trapezoidal rule [34] for numerical integration is applied to the \mathcal{Q} -function which leads to:

$$\mathcal{Q}(\sqrt{x}) = \frac{1}{4n} \exp\left(-\frac{x}{2}\right) + \frac{1}{2n} \sum_{c=1}^{n-1} \exp\left(-\frac{x}{S_c}\right), \quad (3.12)$$

where $S_c = 2 \sin^2(\frac{c\pi}{2n})$ and n is the number of summations. It is shown by Quazi [34] that choosing n greater than 6 results in sufficient accuracy in the numerical integration.

Using Eq. (3.12), Eq. (3.11) can be simplified to:

$$\begin{aligned} P(\mathbf{x}_{k,q} \rightarrow \mathbf{x}_{k,\hat{q}} | \mathbf{H}) &= \mathcal{Q}\left(\sqrt{\sum_{i=1}^{N_r} v_i}\right) \\ &= \frac{1}{4n} \exp\left(-\frac{\sum_{i=1}^{N_r} v_i}{2}\right) + \frac{1}{2n} \sum_{c=1}^{n-1} \exp\left(-\frac{\sum_{i=1}^{N_r} v_i}{S_c}\right) \\ &= \frac{1}{4n} \prod_{i=1}^{N_r} \left(\exp\left(-\frac{v_i}{2}\right)\right) + \frac{1}{2n} \sum_{c=1}^{n-1} \prod_{i=1}^{N_r} \left(\exp\left(-\frac{v_i}{S_c}\right)\right) \end{aligned} \quad (3.13)$$

The PEP conditioned on \mathbf{H} defined in Eq. (3.13) is averaged by integrating over the fading distribution,

$$P(\mathbf{x}_{k,q} \rightarrow \mathbf{x}_{k,\hat{q}}) = \int_0^\infty \mathcal{Q}\left(\sqrt{\sum_{i=1}^{N_r} v_i}\right) P(v_i) dv_i, \quad (3.14)$$

where the Gaussian function, $Q(x)$, is defined above and the fading probability density function (PDF) of v_i is given by [26]:

$$P(v_i) = \frac{1}{\bar{v}_i} \exp\left(-\frac{v_i}{\bar{v}_i}\right), \quad (3.15)$$

where the variance \bar{v}_i is given by:

$$\bar{v}_i = E\left\{\frac{1}{2}|u_i|^2\right\} = E\left\{\frac{1}{2}\left|\sqrt{\frac{\rho}{2}}[h_{i,k_1}d_1 + h_{i,k_2}d_2]e^{j\theta_k}\right|^2\right\} = \frac{\rho}{4}(|d_1|^2 + |d_2|^2), \quad (3.16)$$

where the reader is reminded that $h_{i,k_1}, h_{i,k_2} \sim CN(0, 1)$ as defined in Sec. 3.3. Since the result in Eq. (3.16) show that \bar{v}_i is independent of i , $\bar{v} = \bar{v}_i$ for all $i \in [1 : N_r]$.

Substituting Eq. (3.13) in Eq. (3.14), the unconditional probability can be written as

$$\begin{aligned} P(\mathbf{x}_{k,q} \rightarrow \mathbf{x}_{k,\hat{q}}) &= \int_0^\infty \frac{1}{4n} \prod_{i=1}^{N_r} \left(\exp\left(-\frac{v_i}{2}\right) \right) + \frac{1}{2n} \sum_{c=1}^{n-1} \prod_{i=1}^{N_r} \left(\exp\left(-\frac{v_i}{S_c}\right) \right) P(v_i) dv_i \\ &= \frac{1}{4n} \prod_{i=1}^{N_r} \left(\mathcal{M}\left(\frac{1}{2}\right) \right) + \frac{1}{2n} \sum_{c=1}^{n-1} \prod_{i=1}^{N_r} \left(\mathcal{M}\left(\frac{1}{S_c}\right) \right), \end{aligned} \quad (3.17)$$

where $\mathcal{M}(\cdot)$ is the moment generating function (MGF) for Rayleigh Fading and is defined by [28]:

$$\mathcal{M}(s) = (1 + s\bar{v})^{-1}. \quad (3.18)$$

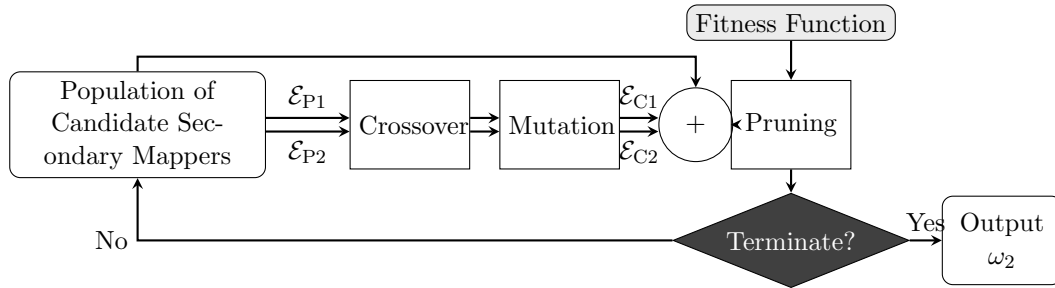
Since, the MGF is independent of i as shown in Eq. (3.18), $\prod_{i=1}^{N_r} \mathcal{M}(s) = [\mathcal{M}(s)]^{N_r}$. Hence, the average BER expression of symbol estimation may be obtained by substituting the unconditioned probability derived in Eq. (3.17) in overall bound defined in Eq. (3.10). The resultant final expression for P_d is as follows:

$$P_d \leq \frac{1}{mM} \sum_{q=0}^{M-1} \sum_{\substack{\hat{q}=0 \\ \hat{q} \neq q}}^{M-1} N(q, \hat{q}) \frac{1}{4n} \left(1 + \frac{\bar{v}}{2}\right)^{-N_r} + \frac{1}{2n} \sum_{c=1}^{n-1} \left(1 + \frac{\bar{v}}{S_c}\right)^{-N_r} \quad (3.19)$$

3.6 Constellation Reassignment Mapper Design

In order to achieve LD, CR requires the use of primary and secondary mappers. For the M -APSK GSM-CR system, primary mapper (ω_1) is designed to follow a Gray coded structure, which is proven to be optimal as discussed by Samra et al [15]. As discussed in Sec. 1, there is no precedence for the design of secondary mappers (ω_2) for the M -APSK constellations considered in this chapter. Thus, the generic approach proposed by Patel et al[23] for LD systems is adopted in this chapter. This approach utilizes a genetic algorithm to design secondary mappers for space-time labelling diversity (STLD) systems. Since both STLD and CR systems require a secondary mapper to achieve LD, this algorithm is adapted and applied for the M -APSK GSM-CR system.

The analytical expressions derived in Sec. 3.5 for the error performance of M -APSK GSM-CR system are used to guide the mapper design process. In particular, since CR only affects the probability of a symbol pair estimation error (P_d), the results of Sec. 3.5.2 form the framework for this design. The first stage of this design is similar to that employed by Xu et al[14], which considers a high SNR approximation of the symbol pair estimation, P_d . At high SNR, the Rayleigh fading MGF (defined in Eq. (3.18)) is dominated by its second term. As such, following on from Eq. (3.19), P_d at high SNR is approximated as



$\mathcal{E}_{P1}, \mathcal{E}_{P2}$ = parent chromosomes. $\mathcal{E}_{C1}, \mathcal{E}_{C2}$ = child chromosomes.

FIGURE 3.3: Block Diagram of Genetic Algorithm for CR Mapper Design

$$P_d^{\text{high SNR}} \leq \frac{1}{mM} \sum_{q=0}^{M-1} \sum_{\hat{q}=0}^{M-1} N(q, \hat{q}) \frac{1}{4n} \left(\frac{\rho}{8} (|d_1|^2 + |d_2|^2) \right)^{-N_r} + \frac{1}{2n} \sum_{i=1}^{n-1} \left(\frac{\rho}{4S_i} (|d_1|^2 + |d_1|^2) \right)^{-N_r}, \quad (3.20)$$

where Eq. (3.16) has been substituted into the expression. It is thus apparent that the performance of the system is dependent on the sum of the squared distances, given by

$$\mathcal{D} = |d_1|^2 + |d_2|^2 = |x_q - x_{\hat{q}}|^2 + |\tilde{x}_q - \tilde{x}_{\hat{q}}|^2. \quad (3.21)$$

Higher values of \mathcal{D} result in lower probability P_d . Thus, the error floor of P_d is set by the minimum value of \mathcal{D} , which is denoted as \mathcal{D}_{\min} . It then follows that the overall objective of mapper design for CR systems is to produce mapper ω_2 given ω_1 in order to maximise \mathcal{D}_{\min} .

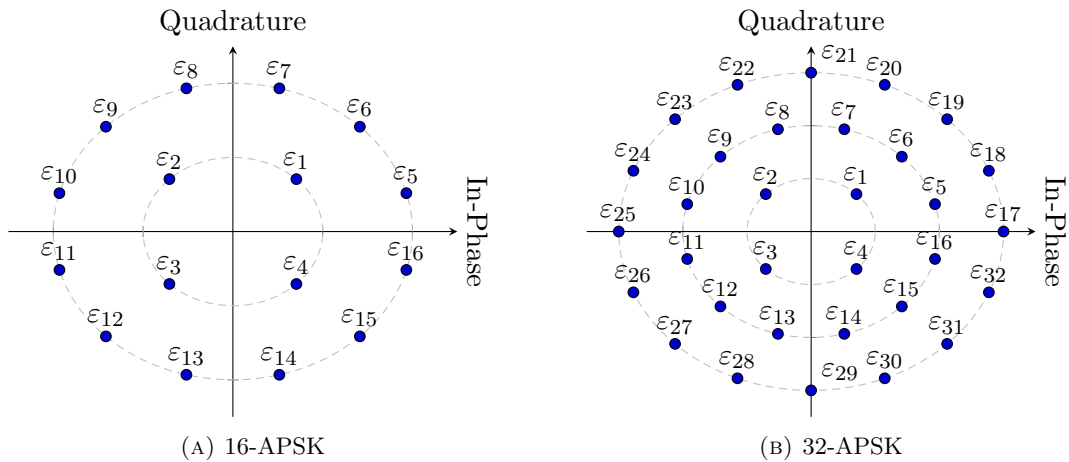
3.6.1 Description of Genetic Algorithm

The genetic algorithm described by Patel et al[23] considers the case where ω_1 is known and ω_2 is desired. The output of this algorithm is obtained from an iterative heuristic search through the candidate mapper space.

The block diagram in Fig. 3.3 provides a high level illustration of the genetic algorithm designed by Patel et al[23]. Candidate secondary mappers are encoded into data structures called ‘chromosomes’, which consist of subunits referred to as ‘genes’. The set of chromosomes considered at each iteration of the algorithm is referred to as the ‘population’. The notation used in this section is to represent genes, chromosomes and the population with variables ε , \mathcal{E} and ϱ respectively.

In the remainder of this section, the authors provide a summarised discussion of each stage of the genetic algorithm.

Genetic Coding ‘Genetic coding’ is the term used to describe the representation of each candidate mapper as a chromosome. Each chromosome consists of genes, ε_i , $i \in [1 : M]$, each of


 FIGURE 3.4: Illustrating the position of Genes in M -APSK Constellations

which corresponds to a symbol from the M -APSK constellation. The corresponding value assigned to each gene of the chromosome is the binary value associated with that constellation point. Thus, the chromosome \mathcal{E} is defined by

$$\mathcal{E} = [\varepsilon_1 \ \varepsilon_2 \ \cdots \ \varepsilon_{M-1} \ \varepsilon_M]. \quad (3.22)$$

An illustration of the 16-APSK and 32-APSK constellations considered in this chapter, explicitly showing the location of each gene, is given in Fig. 3.4.

Generating a Population of Chromosomes The population of chromosomes refers to the set of candidate secondary mappers evaluated by the genetic algorithm at each iteration. Hence, the population during the n -th iteration, ϱ_n , is defined as:

$$\varrho_n = \left\{ \mathcal{E}_{1,n} \ \mathcal{E}_{2,n} \ \cdots \ \mathcal{E}_{(z-1),n} \ \mathcal{E}_{z,n} \right\}, \quad (3.23)$$

where z is the number of chromosomes in the population. As suggested by Patel et al[23], the initial population (ϱ_0) consists of a set of z chromosomes selected at random from the $M!$ candidate mapper space.

Crossover and Mutation The processes of crossover and mutation are the most important elements of the genetic algorithm[35]. Crossover and mutation model the biological process of evolution to generate progressively more optimal population ϱ at each iteration. Hence, the population ϱ_{n+1} is more optimal than ϱ_n .

The κ -point hypersphere swap crossover (κ -HSX) proposed by Patel et al[23] for STLD mapper design is implemented for this genetic algorithm. The authors note that the goal of mapper design in STLD and CR systems are similar, thus no modifications to κ -HSX are needed to apply it in the

CR context. The reader is referred to the original work[23] for full details of the κ -HSX process, including a procedural example of the swapping process.

Mutation is a random event that occurs when a child chromosome undergoes further changes after crossover. The probability of a mutation occurring for a given child chromosome is denoted P_{mutation} . If a mutation occurs, two genes are randomly selected from the child chromosome and swapped. Patel et al[23] highlight that, unlike crossover, no properties from the parent chromosomes are used to inform this swap.

Pruning The purpose of pruning at end of each iteration is to discard the least-fit chromosomes from the population. This is done to model the biological process of ‘natural selection’. In the genetic algorithm for mapper design, $2 \times \binom{z}{2}$ chromosomes are discarded at the end of each iteration. In this way, the population size at the start of each iteration remains fixed at z . When pruning the population, a metric to quantitatively evaluate chromosomes is necessary. As mentioned previously, the error floor of the symbol pair estimation probability of the GSM-CR system is set by the minimum summed-squared distance, \mathcal{D}_{\min} . This suggests that an appropriate fitness function to evaluate chromosome \mathcal{E} when pruning is given by

$$\Psi(\mathcal{E}) = \min_{q, \hat{q} \in [0:M-1]} \{ |x_q - x_{\hat{q}}|^2 + |\omega_{\mathcal{E}}(q) - \omega_{\mathcal{E}}(\hat{q})|^2 \}, \quad (3.24)$$

where $\omega_{\mathcal{E}}$ is the mapper represented by chromosome \mathcal{E} . Eq. (3.24) is obtained from Eq. (3.21) by obtaining \tilde{x}_q and $\tilde{x}_{\hat{q}}$ from $\omega_{\mathcal{E}}$. Thus, the z chromosomes with the highest fitness, evaluated using Eq. (3.24), form the population ϱ_{n+1} at the end of the pruning stage.

The authors emphasise that the fitness function in Eq. (3.24) is the key difference between the genetic algorithm for CR systems and its original variant for STLD systems[23].

Termination Termination of a genetic algorithm occurs when the population is deemed to contain an optimal solution, or if the algorithm determines that no feasible solution can be found.

As suggested by Patel et al[23], the population is said to contain an optimal solution when all chromosomes converge to the same genotype (i.e. they all have the same fitness). All chromosomes in the population are then considered equally optimal, and any of them may be selected as the output.

Patel et al[23] also constrain the algorithm to run for a maximum of n_{\max} iterations to ensure that it is computationally feasible, where $n_{\max} \ll M^5$. If the maximum number of iterations is reached, it is assumed that the genetic algorithm will not converge. In this case, the fittest chromosome from the population is selected as the output.

TABLE 3.1: PAPR of M -APSK and M -QAM constellations

	16-APSK	16-QAM	32-APSK	32-QAM
PAPR (dB)	1.1	2.6	1.9	3.2

Implementation When implementing the algorithm to produce secondary mappers for the context of CR for 16-APSK and 32-APSK constellations, the following parameters were used: $z = 8$ and $P_{\text{mutation}} = 0.1$. The κ -HSX algorithm is implemented with parameter $\kappa = \frac{M-4}{2}$. The maximum number of iterations for the GA is set to $n_{\text{max}} = 10^4$ for 16-APSK and $n_{\text{max}} = 10^6$ for 32-APSK constellation.

3.7 Results and Discussion

The section begins with a discussion of the PAPR comparison between M -APSK constellations and the more widely used M -QAM constellations. The values for M -APSK and M -QAM PAPR were obtained using Eq. (3.7) and are shown in Table. 3.1. It is clearly evident that the lower number of amplitude levels in APSK constellations results in a lower PAPR when compared to QAM[12]. This characteristic of APSK constellations justifies its adoption in long-range wireless communication systems. This motivates for the application of M -APSK constellations to advance SM systems such as GSM and GSM-CR in this chapter. Consequently, the performance study of the proposed M -APSK GSM and M -APSK GSM-CR systems is presented in what follows.

The performance of the proposed systems is presented in terms of the average BER analytical expression developed in Sec. 3.5. These results are validated using Monte Carlo simulations for various antenna array sizes and configurations. Thereafter, performance comparisons are made

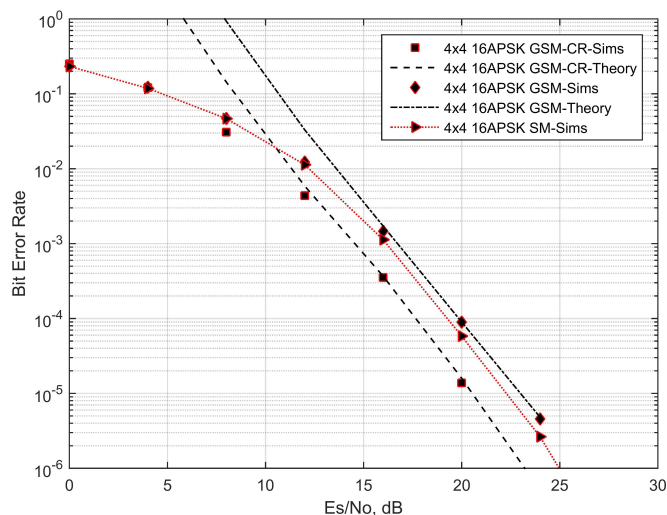


FIGURE 3.5: Average BER - 6 bits/s/Hz Configuration

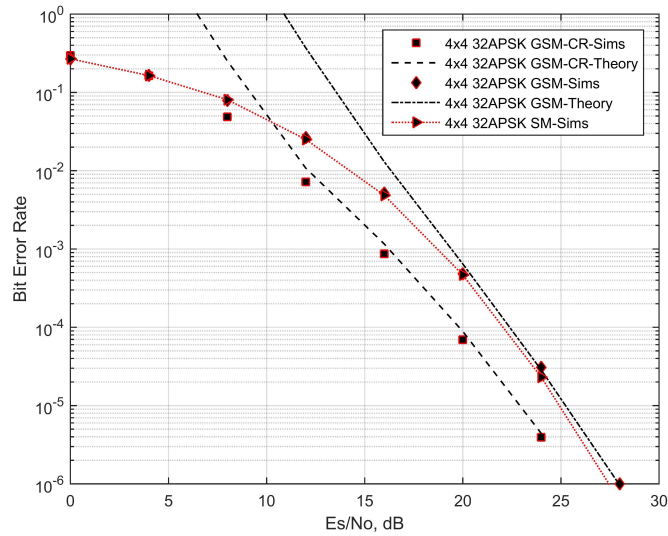


FIGURE 3.6: Average BER - 7 bits/s/Hz Configuration

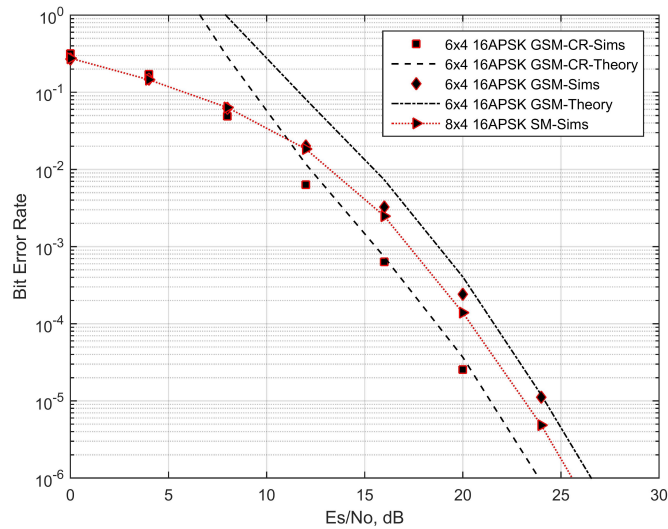


FIGURE 3.7: Average BER - 7 bits/s/Hz Configuration

between SM, GSM and GSM-CR systems with equivalent spectral efficiencies. In the performance study, assume $N_r = 4$ and that the channel remains constant for the duration of a single transmission.

Monte Carlo simulations were performed using the ML detection rule defined in Eq. (3.4) with the following assumptions: Rayleigh flat fading channel, full knowledge of channel at the receiver, the

 TABLE 3.2: $4 \times N_r$ Antenna Pairs

Antenna array sizes and configurations	$4 \times N_r$			
	(1,3)	(1,4)	(2,3)	(2,4)
Transmit Antenna Pair	(1,3)	(1,4)	(2,3)	(2,4)
Rotation Angle (16-APSK)	0	$\pi/4$	$\pi/4$	0
Rotation Angle (32-APSK)	0	$\pi/4$	$\pi/4$	0

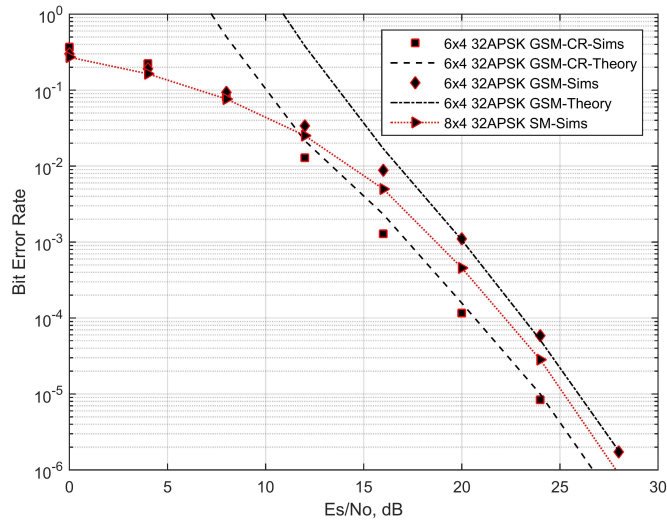


FIGURE 3.8: Average BER - 8 bits/s/Hz Configurations

 TABLE 3.3: $6 \times N_r$ Antenna Pairs

Antenna array sizes and configurations	$6 \times N_r$							
Transmit Antenna Pair	(1,2)	(3,4)	(5,6)	(2,3)	(4,5)	(1,6)	(1,3)	(2,4)
Rotation Angle (16-APSK)	0	0	0	$\pi/3$	$\pi/3$	$\pi/3$	$2\pi/3$	$2\pi/3$
Rotation Angle (32-APSK)	0	0	0	$\pi/6$	$\pi/6$	$\pi/6$	$\pi/3$	$\pi/3$

antennas at the transmitter and receiver are separated wide enough to avoid correlation, maximal ratio combining reception is used at the receiver and the total transmit power is split equally between the two active transmit antennas. Rotation angles and the selection of the transmit antenna pairs are based on the design proposed by Basar et al [9]. The transmit antenna pairs used for M -APSK GSM and M -APSK GSM-CR were obtained from Basar et al for a $4 \times N_r$ and $6 \times N_r$ and shown in Table 3.2 and Table 3.3 respectively [9]. Since it is not possible to derive rotation angles for $M > 4$ [9], an exhaustive search via computer simulation is conducted to maximize the average BER performance. The results obtained are outlined in Table 3.2 and Table 3.3. Fig. 3.5-3.8 show the average BER of SM, GSM and GSM-CR with various AASC. In order to ensure a fair comparison, identical spatial mappings were employed for both GSM and GSM-CR systems. The simulation results for all cases of GSM and GSM-CR systems are observed to converge the union bound in high SNR region thus verifying the analytical average BER expressions derived in Sec. 3.5. It is also evident that in all cases, the GSM-CR outperforms the GSM and SM systems. Fig. 3.5 and Fig. 3.6 show the average BER for 4×4 antenna configuration for 16-APSK and 32-APSK respectively. These correspond to spectral efficiencies of 6 bits/s/Hz and 7 bits/s/Hz respectively. As the graphs in Fig. 3.5 show, the 16-APSK GSM-CR system achieves the gain of 2.5 dB over its equivalent GSM system and 1.5 dB in comparison to its equivalent SM system at BER of 10^{-5} . Furthermore, GSM systems are shown to have slightly degraded performance in comparison to SM. The higher error probability of detecting two transmit antennas in GSM, in comparison to the single transmit antenna detection in SM, is the reason for the degraded performance [5]. In Fig. 3.6, the 32-APSK

GSM-CR systems achieves gains of 2.2 dB and 2 dB at BER of 10^{-5} in comparison to its equivalent GSM and SM systems respectively. Fig. 3.7 and Fig. 3.8 show the average BER for 6×4 antenna configuration for 16-APSK and 32-APSK respectively. These correspond to spectral efficiencies of 7 bits/s/Hz and 8 bits/s/Hz respectively. It can be seen in Fig. 3.7 that the 16-APSK GSM-CR system achieves the gain of 2.5 dB over its equivalent GSM system and 1.5 dB in comparison to its equivalent SM system at BER of 10^{-5} . In Fig. 3.8, the 32-APSK GSM-CR systems achieves gains of 2 dB and 1.2 dB at BER of 10^{-5} in comparison to its equivalent GSM and SM systems respectively. It should be noted that similar performance improvements were observed in *M*-QAM GSM-CR over SM and GSM in the original work done by Naidoo et al[13].

The performance gains for the *M*-APSK GSM-CR system over the *M*-APSK GSM system in various AASC is attributed to the improved error performance of symbol pair estimation, P_d . This is due to the introduction of labelling diversity in the system. Since, P_d has been significantly improved, using Eq. (3.8), it can be concluded that the overall probability of the system is now bounded by P_a if P_d approaches 0. Hence, for future works, the next logical step would be to improve the average BER of transmit antenna pair estimation, P_a , in order to further improve link reliability of GSM systems.

3.8 Conclusion

This chapter presents a performance study of an *M*-APSK GSM-CR system. An analytical framework for the average BER is formulated for the *M*-APSK GSM-CR system. The framework guides the design of the genetic algorithm used to develop secondary mappers for APSK. The first set of results focus on a PAPR comparison between *M*-APSK constellations to *M*-QAM. As expected, the APSK constellations achieve a lower PAPR as compared to QAM. The second set of results focus on validating the theoretical expression derived by the results of Monte Carlo simulations, which show a tight bound in the high SNR region. The results presented further show that the *M*-APSK GSM-CR outperforms its equivalent GSM and SM systems in various antenna array sizes and configurations. A 4×4 16-APSK GSM-CR systems achieves gains of 2.5 dB over its equivalent GSM system and 1.5 dB in comparison to its equivalent SM system at BER of 10^{-5} . Similar gains are evident for 32-APSK and at various spectral efficiencies.

3.9 Future Works

The findings from this chapter opens up the possibility of future research work to be done in multiple areas. Firstly, the error performance may be improved by application of more recent APSK constellations with the novel GSM-CR system. The NE-APSK constellations [21] is one such constellation that may be considered for the proposed system. The generic mapper design detailed in

this chapter allows the system to generate secondary mappers for any type and size of constellations. Secondly, this chapter shows that the GSM-CR system is bound by the error probability of antenna pair estimation. The future work should focus on enhancing P_a to further improve the link reliability of GSM and GSM-CR systems. Lastly, there are more advanced SM systems that further improve performance when compared GSM-CR such as Space-Time Quadrature Spatial Modulation (ST-QSM), Generalised QSM (GQSM) and Extended QSM (EQSM) [36–38]. In future work, the authors will consider the application of circular constellations to such systems.

3.10 Appendix: Derivation of the Q-function Derivation

In this section, the derivation of the Q-function for the proposed system is shown.

Rewriting using alternative notation shown in Eq. (3.3) yields:

$$\begin{aligned}
 P(\mathbf{x}_{k,q} \rightarrow \mathbf{x}_{k,\hat{q}} | \mathbf{H}) &= P\left(\left\|\sqrt{\frac{\rho}{2}}\mathbf{h}_k[\mathbf{X}_q - \mathbf{X}_{\hat{q}}] + \mathbf{n}\right\|_F^2 < \|\mathbf{n}\|_F^2\right) \\
 &= P\left(\left\|\sqrt{\frac{\rho}{2}}\left[\mathbf{h}_{k_1}(x_q - x_{\hat{q}})e^{j\theta_k} + \mathbf{h}_{k_2}(\tilde{x}_q - \tilde{x}_{\hat{q}})e^{j\theta_k}\right] + \mathbf{n}\right\|_F^2 < \|\mathbf{n}\|_F^2\right) \\
 &= P\left(\left\|\sqrt{\frac{\rho}{2}}\left[\mathbf{h}_{k_1}d_1 + \mathbf{h}_{k_2}d_2\right]e^{j\theta_k} + \mathbf{n}\right\|_F^2 < \|\mathbf{n}\|_F^2\right), \tag{3.25}
 \end{aligned}$$

where $d_1 = (x_q - x_{\hat{q}})$ and $d_2 = (\tilde{x}_q - \tilde{x}_{\hat{q}})$.

Let $\mathbf{u} = \sqrt{\frac{\rho}{2}}[\mathbf{h}_{k_1}d_1 + \mathbf{h}_{k_2}d_2]e^{j\theta_k}$, the PEP in Eq. (3.25) can be resolved to:

$$\begin{aligned}
 P(\mathbf{x}_{k,q} \rightarrow \mathbf{x}_{k,\hat{q}} | \mathbf{H}) &= P\left(\|\mathbf{u} + \mathbf{n}\|_F^2 < \|\mathbf{n}\|_F^2\right) \\
 &= P\left(\|\mathbf{u}\|_F^2 + 2\Re(\mathbf{n}^H\mathbf{u}) < 0\right) \\
 &= P\left(\sum_{i=1}^{N_r}\Re(n_i^*u_i) > \frac{\sum_{i=1}^{N_r}|u_i|^2}{2}\right), \tag{3.26}
 \end{aligned}$$

where n_i and u_i are the i^{th} element of vectors \mathbf{n} and \mathbf{u} respectively.

From the definition of AWGN in Sec. 3.3, n_i follows the distribution given by $n_i \sim CN(0, 1)$, where $i \in [1 : N_r]$. In addition, $n_i^*u_i$ is also a complex Gaussian random variable due to the conditional PEP in Eq. (3.25) assuming perfect knowledge of all channels. Therefore, $\Re(n_i^*u_i)$ is a Gaussian random variable with zero mean and variance $\sigma_i^2 = \frac{|u_i|^2}{2}$.

Dividing both sides of the conditional probability by the square root of the variance, yields an expression in terms of the definition of the Gaussian \mathcal{Q} -function [33], $\mathcal{Q}(x) = \frac{1}{\pi} \int_0^{\frac{\pi}{2}} \exp\left(-\frac{x}{2\sin^2(y)}\right) dy$, as follows:

$$\begin{aligned}
 P(\mathbf{x}_{k,q} \rightarrow \mathbf{x}_{k,\hat{q}} | \mathbf{H}) &= P\left(\sum_{i=1}^{N_r} \frac{\Re(n_i^* u_i)}{\sigma_i} > \frac{1}{2} \sum_{i=1}^{N_r} \frac{|u_i|^2}{\sigma_i}\right) \\
 &= \mathcal{Q}\left(\sqrt{\sum_{i=1}^{N_r} \frac{|u_i|^2}{2}}\right) \\
 &= \mathcal{Q}\left(\sqrt{\sum_{i=1}^{N_r} v_i}\right), \tag{3.27}
 \end{aligned}$$

where $v_i = \frac{|u_i|^2}{2}$.

References

- [1] G. J. Foschini, “Layered space-time Architecture for Wireless Communication in a Fading Environment When Using multi-element Antennas,” *Bell Labs Technical Journal*, vol. 1, no. 2, pp. 41–59, Aug. 2002, doi: 10.1002/bltj.2015.
- [2] P. W. Wolniansky, G. J. Foschini, G. D. Golden, and R. A. Valenzuela, “V-BLAST: An Architecture for Realizing Very High Data Rates over the rich-scattering Wireless Channel,” in *1998 URSI International Symposium on Signals, Systems, and Electronics. Conference Proceedings (Cat. No.98EX167)*, 2002, pp. 295–300.
- [3] S. M. Alamouti, “A Simple Transmit Diversity Technique for Wireless Communications,” *IEEE Journal on Selected Areas in Communications*, vol. 16, no. 8, pp. 1451–1458, 1998, doi: 10.1109/49.730453.
- [4] R. Y. Mesleh, H. Haas, S. Sinanovic, Chang Wook Ahn, and Sangboh Yun, “Spatial Modulation,” *IEEE Transactions on Vehicular Technology*, vol. 57, no. 4, pp. 2228–2241, Jul. 2008, doi: 10.1109/tvt.2007.912136.
- [5] A. Younis, N. Serafimovski, R. Mesleh, and H. Haas, “Generalised Spatial Modulation,” in *2010 Conference Record of the Forty Fourth Asilomar Conference on Signals, Systems and Computers*, Nov. 2010, pp. 1498–1502.
- [6] N. Ma, A. Wang, C. Han, and Y. Ji, “Adaptive Joint Mapping Generalised Spatial Modulation,” in *2012 1st IEEE International Conference on Communications in China (ICCC)*, Nov. 2012, pp. 520–523.
- [7] Z. Yiğit and E. Başar, “High-rate Generalized Spatial Modulation,” in *2016 24th Signal Processing and Communication Application Conference (SIU)*, Jun. 2016, pp. 1117–1120.
- [8] Y. Zhou, D. Yuan, X. Zhou, and H. Zhang, “Trellis Coded Generalized Spatial Modulation,” in *2014 IEEE 79th Vehicular Technology Conference (VTC Spring)*, Jan. 2015, pp. 1–5.
- [9] E. Basar, U. Aygolu, E. Panayirci, and H. V. Poor, “Space-Time Block Coded Spatial Modulation,” *IEEE Transactions on Communications*, vol. 59, no. 3, pp. 823–832, Mar. 2011, doi: 10.1109/tcomm.2011.121410.100149.
- [10] K. Sundaravadivu and S. Bharathi, “STBC Codes for Generalized Spatial Modulation in MIMO Systems,” in *2013 IEEE International Conference On Emerging Trends in Computing, Communication and Nanotechnology (ICECCN)*, Jun. 2013, pp. 486–490.
- [11] K. Govindasamy, H. Xu, and N. Pillay, “Space-time block coded spatial modulation with labeling diversity,” *International Journal of Communication Systems*, vol. 31, no. 1, p. e3395, Sep. 2017, doi: 10.1002/dac.3395.

- [12] M. Baldi, F. Chiaraluce, A. de Angelis, R. Marchesani, and S. Schillaci, "A Comparison between APSK and QAM in Wireless Tactical Scenarios for Land Mobile Systems," *EURASIP Journal on Wireless Communications and Networking*, vol. 2012, no. 1, Oct. 2012, doi: 10.1186/1687-1499-2012-317.
- [13] N. Naidoo, "Enhanced Performance and Efficiency Schemes for Generalised Spatial Modulation," PhD Thesis, University of KwaZulu-Natal, 2017.
- [14] H. Xu, K. Govindasamy, and N. Pillay, "Uncoded Space-Time Labeling Diversity," *IEEE Communications Letters*, vol. 20, no. 8, pp. 1511–1514, Aug. 2016, doi: 10.1109/lcomm.2016.2580503.
- [15] H. Samra, Z. Ding, and P. M. Hahn, "Symbol Mapping Diversity Design for Multiple Packet Transmissions," *IEEE Transactions on Communications*, vol. 53, no. 5, pp. 810–817, May 2005, doi: 10.1109/tcomm.2005.847132.
- [16] K. G. Seddik, A. S. Ibrahim, and K. J. Ray Liu, "Trans-Modulation in Wireless Relay Networks," *IEEE Communications Letters*, vol. 12, no. 3, pp. 170–172, Mar. 2008, doi: 10.1109/lcomm.2008.071734.
- [17] T. Quazi and H. Xu, "BER Performance of a Hierarchical APSK UEP System over Nakagami-m Fading," *SAIEE Africa Research Journal*, vol. 107, no. 4, pp. 230–236, Dec. 2016, doi: 10.23919/saiee.2016.8532258.
- [18] European Telecommunications Standards Institute, Digital Video Broadcasting (DVB); *Second Generation Framing structure, Channel Coding and Modulation Systems for Broadcasting, Interactive Services, News Gathering and Other Broadband Satellite Applications*. France: European Broadcasting Union, 2014.
- [19] P. A. Martin, "Differential Spatial Modulation for APSK in Time-Varying Fading Channels," *IEEE Communications Letters*, vol. 19, no. 7, pp. 1261–1264, Jul. 2015, doi: 10.1109/lcomm.2015.2426172.
- [20] Y. Zhou, H. Zhang, P. Zhang, and D. Yuan, "Non-Coherent Spatial Modulation and Optimal Multi-Ring APSK Constellation Design," *IEEE Communications Letters*, vol. 22, no. 5, pp. 950–953, May 2018, doi: 10.1109/lcomm.2018.2810876.
- [21] F. Yang, K. Yan, Q. Xie, and J. Song, "Non-Equiprobable APSK Constellation Labeling Design for BICM Systems," *IEEE Communications Letters*, vol. 17, no. 6, pp. 1276–1279, Jun. 2013, doi: 10.1109/lcomm.2013.050313.130306.
- [22] K. Yan, F. Yang, C. Pan, J. Song, F. Ren, and J. Li, "Genetic Algorithm Aided gray-APSK Constellation Optimization," in *2013 9th International Wireless Communications and Mobile Computing Conference (IWCMC)*, Aug. 2013, pp. 1705–1709.

- [23] S. S. Patel, T. Quazi, and H. Xu, "A Genetic Algorithm for Designing Uncoded Space-Time Labelling Diversity Mappers," in *2018 IEEE International Workshop on Signal Processing Systems (SiPS)*, 2019, pp. 1–6.
- [24] S. Patel, "Uncoded Space-Time Labelling Diversity: Data Rate and Reliability Enhancements and Application to Real-World Satellite Broadcasting," PhD Thesis, University of KwaZulu-Natal, 2019.
- [25] H. G. Myung and D. J. Goodman, *Single Carrier FDMA a New Air Interface for Long Term Evolution*. Chichester, Uk John Wiley & Sons, Ltd, 2008.
- [26] A. Goldsmith, *Wireless Communications*. Cambridge: Cambridge University Press, 2005.
- [27] J. G. Proakis, *Digital Communications*, 4th ed. Boston: Mcgraw-Hill, 2001.
- [28] Marvin Kenneth Simon and Mohamed-Slim Alouini, *Digital Communication over Fading Channels*. Hoboken, N.J.: Wiley-Interscience, 2005.
- [29] W. Sung, S. Kang, P. Kim, D.-I. Chang, and D.-J. Shin, "Performance Analysis of APSK Modulation for DVB-S2 Transmission over Nonlinear Channels," *International Journal of Satellite Communications and Networking*, vol. 27, no. 6, pp. 295–311, May 2009, doi: 10.1002/sat.938.
- [30] J.-H. Kim, C. S. Sin, S. U. Lee, and J. H. Kim, "Improved Performance of APSK Modulation Scheme for Satellite System," in *2007 6th International Conference on Information, Communications & Signal Processing*, 2008, pp. 1–4.
- [31] H. Alasady and M. Ibnkahla, "Adaptive Modulation over Nonlinear time-varying Channels," in *2005 12th IEEE International Conference on Electronics, Circuits and Systems*, 2008, pp. 1–4.
- [32] R. De Gaudenzi, A. Guillen i Fabregas, and A. Martinez, "Performance Analysis of turbo-coded APSK Modulations over Nonlinear Satellite Channels," *IEEE Transactions on Wireless Communications*, vol. 5, no. 9, pp. 2396–2407, Sep. 2006, doi: 10.1109/twc.2006.1687763.
- [33] J. W. Craig, "A new, Simple and Exact Result for Calculating the Probability of Error for two-dimensional Signal Constellations," in *MILCOM 91 - Conference Record*, 2002, pp. 571–575.
- [34] T. Quazi, "Cross-layer Design for the Transmission of Multimedia Traffic over Fading Channels," PhD Thesis, University of KwaZulu-Natal, 2009.
- [35] Z. H. Ahmed, "An Improved Genetic Algorithm Using Adaptive Mutation Operator for the Quadratic Assignment Problem," in *2015 38th International Conference on Telecommunications and Signal Processing (TSP)*, 2015, pp. 1–5.
- [36] Z. Yiğit and E. Başar, "Space-time Quadrature Spatial Modulation," in *2017 IEEE International Black Sea Conference on Communications and Networking (BlackSeaCom)*, 2018, pp. 1–5.

- [37] F. R. Castillo-Soria, J. Cortez, C. A. Gutiérrez, M. Luna-Rivera, and A. Garcia-Barrientos, “Extended Quadrature Spatial Modulation for MIMO Wireless Communications,” *Physical Communication*, vol. 32, pp. 88–95, Feb. 2019, doi: 10.1016/j.phycom.2018.11.006.
- [38] R. Mesleh, S. S. Ikki, and H. M. Aggoune, “Quadrature Spatial Modulation,” *IEEE Transactions on Vehicular Technology*, vol. 64, no. 6, pp. 2738–2742, Jun. 2015, doi: 10.1109/tvt.2014.2344036.

Chapter 4

Conclusion

The primary objective of this dissertation was to apply circular constellations to advanced MIMO systems such as SM, GSM and GSM-CR. These advanced systems were previously only applied to square or rectangular modulation schemes. Various benefits and applications of circular constellations have been discussed at length in this dissertation. The principal contributions and corresponding outcomes are summarised as follows:

In Chapter 2, the focus was to develop a closed form of the average BER theoretical expression for the 16-APSK SM and the 32-APSK SM systems. The theoretical expressions derived herein were used to verify the simulation results published previously. The performance study was then extended in this chapter to include results of various AASC for the M -APSK SM system. The average BER theoretical expressions derived were shown to have a tight bound to the simulation results in the high SNR region for these various AASC.

Chapter 3 proposed an M -APSK GSM and M -APSK GSM-CR systems in order to increase the spectral efficiency and link reliability of M -APSK SM systems. The M -APSK GSM system, compared to M -APSK SM, improves the overall spectral efficiency by $\log_2(N_c)$, where N_c is the number of antenna combinations. Although the spectral efficiency is significantly improved as the number of transmit antennas increase, the BER performance of the GSM system is limited compared to SM. Therefore, an M -APSK GSM-CR system was developed to improve the overall link reliability of the conventional GSM system. The results presented show that the M -APSK GSM-CR system outperforms its equivalent GSM and SM systems for various AASC. A 4×4 16-APSK GSM-CR system achieved gains of 2.5dB over its equivalent GSM system and 1.5dB in comparison to its equivalent SM system at BER of 10^{-5} . Similar gains were evident for 32-APSK and at various different spectral efficiencies. Furthermore, an analytical framework for the average BER for the proposed M -APSK GSM and M -APSK GSM-CR system was developed in this chapter. The theoretical expression derived was validated by the results of Monte Carlo simulations, which show a tight bound in the high SNR region.

This dissertation paves the way for future research work to be conducted in multiple areas which includes the following:

1. Application of more advanced circular constellations such as NE-APSK with the novel GSM-CR system to improve the overall link reliability of the M -APSK GSM-CR system. The generic mapper design detailed in this paper allows the system to generate secondary mappers for any type and size of constellations.
2. Application of circular constellations to more advanced SM systems such as ST-QSM, GQSM and EQSM. These systems foundationally transmit the in-phase and quadrature symbols of a signal independently to achieve a superior error performance.
3. Developing a low complexity detector scheme for the M -APSK GSM-CR system which reduces computational complexity regardless of the order of digital modulation employed.